TAMPERE UNIVERSITY OF TECHNOLOGY

MIKHAIL GERASIMENKO

PROTOCOL-LEVEL SIMULATIONS OF MASSIVE MEDIUM ACCESS FOR MACHINE-TYPE COMMUNICATIONS

Master's Thesis

Examiners: Prof. Yevgeni Koucheryavy
and
Dr. Sergey Andreev
Examiners and topic approved in the Faculty of Computing and Electrical Engineering Council meeting on 05.12.2012

ABSTRACT

TAMPERE UNIVERSITY OF TECHNOLOGY
Master's Degree Program in Information Technology
GERASIMENKO, MIKHAIL : Protocol-Level Simulations of Massive Medium Access for Machine-Type Communications
Master of Science Thesis, 47 pages, 0 Appendix pages
November 2013
Major subject: Communications Engineering
Examiners: Prof. Yevgeni Koucheryavy and Dr. Sergey Andreev
Keywords: Machine-Type Communications, Long Term Evolution, Internet of Things, Physical Random Access Channel, System-Level Simulator, overload control

In recent years, Machine-Type Communications (MTC) has become one of the most attractive technologies in the area of wireless networking. Different sources are predicting a large grow of smart grid machine-to-machine deployments in several decades, which also means that the total number of wireless devices will increase dramatically. In connection to this problem, the choice of the standard, which will satisfy all the MTC requirements without harming current wireless deployments has become very relevant. Because of these reasons, many companies are proposing to modify one (or several) of the current wireless standard in a way that it will be possible to use for MTC purposes. This will be perfect from point of view of interference problems, because they will be already included in a standard itself.

Third Generation Partnership Project (3GPP) Long Term Evolution-Advanced (LTE-A) is one of the most rapidly developing wireless technologies, that seems to be an ideal candidate for future MTC implementation. However, while the capacity of typical LTE-A network should be enough to satisfy traffic demands of large number of MTC devices, the signaling is not ready to face new requirements. In this Thesis, we are considering and partly solving problems, that could occur in LTE-A signaling channels under MTC conditions. Particularly, these are data access mechanisms, which could be realized via Physical Uplink Control Channel (PUCCH) and Physical Random Access Channel (PRACH). Speaking about assessment methods, the research made in this work is based on 2 approaches: simulation and analysis. Both of them are also in details described in the pages of this Thesis. As a conclusion it could be said that PUCCH channel is not suitable for the MTC data access, while PRACH is having problems only in heavily loaded (overloaded) cases and should be slightly modified to face them.

PREFACE

The research made in this Thesis was supported by TEKES as part of the Internet of Things program of DIGILE (Finnish Strategic Centre for Science, Technology and Innovation in the field of ICT and digital business) and was completed in collaboration with Ericsson (Finland). Initially, research started in 2012 and it is still ongoing. I hope that the analytical and simulation base, constructed in this Thesis will help us to solve much more difficult problems and will facilitate a high quality follow-up work in the future.

I would like to thank all my colleagues and friends from Tampere University of Technology (TUT) for help and collaboration in the work presented in this Thesis. First of all, I would like to thank Dr. Sergey Andreev and Prof. Yevgeni Koucheryavy, who were guiding and supervising me during my work and study process. Of course, this work has never been completed without help of Olga Galinina and Vitaly Petrov, who were doing a significant part of simulations and analysis. Also, I am very grateful to our colleagues from Ericsson (Finland) Anna Larmo, Tuomas Tirronen, Johan Torsner, for their timely advices, help and sensitive supervision. In addition to this, I would like to thank University of Nizhny Novgorod Wireless Competence Center, especially Alexey Trushanin, Vyacheslav Shumilov and Roman Maslennikov, for their help and collaboration in the "SLS tools overview" part of the Thesis. Finally, I would like to say thank you to Anastasiaa Voropaeva, Alex Pyattaev, Oleg Dementiev, Dmitri Moltchanov, as well as other colleagues, friends and family members, who were giving me inspiration and helping me to make this important step in my life.

I dedicate this Thesis to my grandmother, who was guiding me through my childhood and gave me the best life lessons I ever had.

23.10.2013

MIKHAIL GERASIMENKO

CONTENTS

TERMS, ACRONYMS AND SYMBOLS

ALOHA	Network protocol
BI	Backoff Indicator. Number, indicating the value of backoff for RA procedure
BLER	Block Error Rate. Ratio of error data blocks to total number of data blocks
CDF	Cumulative distribution function. Function, that describes the probability of X to be lower or equal x, where X is a random variable with given probability distribution and x describes x-axis values
CDMA	Code Division Multiple Access. Method of channel access, where division of the channels is made based on multiplication of user data with different pseudo-random coding sequences
DL	Downlink. Direction of data transmission from base station to the users
eNodeB	Evolved Node B. 4G Evolution of NodeB (3G) (base station) element
ETSI	European Telecommunications Standards Institute. Telecommunications standardization organization
EPC	Evolved Packet Core. LTE core, consists of several entities: Mobility Management Entity, Serving Gateway, PDN Gateway, Home Subscriber Server, Access Network Discovery and Selection Function and Evolved Packet Data Gateway
EUTRAN	Evolved Universal Terrestrial Radio Access Network. Radio access part of LTE network
FDD	Frequency Division Duplex. Method of UL and DL channels division. Based on their frequency separation
FSM	Finite State Machine. Mathematical model which is used to describe program logic
GSM	Global System for Mobile Communications. Standard describing second generation cellular networks
HARQ	Hybrid automatic repeat request. Combination of automatic repeat request and forward error correction mechanisms. Target to prevent and/or resend unsuccessful packet

H2H	Human-to-Human communications. Type of wireless communications between two or more UEs, directly controlled by humans
IoT	Internet of things. The concept of an internet-like network, where basic network units are machine-based devices
ITU	International Telecommunication Union. International agency, responsible for telecommunications
LTE	Long Term Evolution. Wireless cellular standard of 4th generation (4G). Starting from release 10, called LTE-Advanced (LTE-A)
L2S	Link-to-System mapping. Link-Layer Simulator results mapping to System-Layer-simulator
MTC	Machine Type Communications. Type of wireless communications between two or more machine-based devices
M2M	Machine-to-Machine. In this context is similar to MTC
OFDMA	Orthogonal Frequency Division Multiple Access. Method of channel access, channels are divided by frequency subcarriers sets
PLS	Protocol-Level Simulator. Less detailed (than SLS) simulator, which main purpose is to simulate certain protocol details
PDCCH	Physical Downlink Control Channel. LTE control channel, used for DL signaling information
PDSCH	Physical Downlink Shared Channel. LTE data channel, used for user DL data transmission
PRACH	Physical Random Access Channel. LTE control channel, initially used for network entry
PUCCH	Physical Uplink Control Channel. LTE control channel, used for UL signaling information
PUSCH	Physical Uplink Shared Channel. LTE data channel, used for user UL data transmission
RA	Random Access procedure. LTE procedure, initially used for network entry.
RAR	Random Access response (Msg2). Message, in which eNodeB answers to the UE Msg1 (RA preamble)

RAN	Radio Access Network. Part of cellular network, which main purpose is to provide connection to user
RB	Resource Block. LTE channel allocation unit
RRC	Radio Resource Control. UMTC protocol stack
RSRQ	Reference Signal Received Quality. LTE Reference signal quality measurement value
RSRP	Reference Signal Received Power. LTE Reference signal power on the receiver side
SINR	Signal to Interference plus Noise Ratio. Value, describing how much signal level is higher than a combination of noise and interference levels
SLS	System-Level Simulator. Simulator, which main goal is to show how network will work in environment close to real
SR	Scheduling Request. Special message UE sends to ask eNodeB for resources.
UE	User Equipment. Mobile user device, used in communication purposes
UL	Uplink. Direction of data transmission from user to base station
UMTS	Universal Mobile Telecommunications System. 3G wireless communications standard
WiMAX	Worldwide Interoperability for Microwave Access. 4G wireless communications standard
3G	3rd Generation. A set of wireless cellular standards, which satisfy certain requirements.
4G	4th Generation
802.16	Series of wireless standards

1. INTRODUCTION

1.1 Structure of the Thesis

Analysis of Long Term Evolution-Advanced (LTE-A) as a candidate technology for Machine-Type Communications (MTC) is large and complicated research task. Therefore, in this Thesis we are touching only small part of the problem, which is mostly related to the signaling channels and associated procedures. However, due to the importance and complexity of the task, several different research instruments were created during this work. In the Chapters of this Thesis we will describe these instruments as well as the research made around the considered problem.

The Thesis is organized as follows: in the rest of Chapter 1 we explain the scope of the Thesis, together with related literature. After that, in Chapter 2 we are introducing the structure, basic parameters and properties of LTE-A. Further in the Chapter 2, the LTE-A access channels are considered, as well as the possible problems that could occur with them under MTC conditions. Chapter 3 is mostly related to the assessment methods used in this Thesis. Here, the advantages and disadvantages of different simulation and mathematical network abstraction mechanisms are considered on the practical examples. In Chapter 4, parameters, assumptions and targeted metrics are given. Description and calibration of the constructed simulator and analysis are also presented in there. In Chapter 5, numerical results are provided and conclusion is made. Finally, it is need to mention, that the results of this research were also published in [1; 2; 3; 4].

1.2 Scope of the Thesis

MTC, also known as Machine-to-Machine (M2M), have recently developed into a critical technology that is expected to generate significant revenues. Industry reports indicate the considerable potential of the MTC market, with millions of devices connected within the following years resulting in predicted revenues of up to $300 billion [5]. According to [6], the concept of MTC broadly enables a device (smart meter, actuator, or sensor) to capture a specific event and relay it through the underlying network to the associated application, which in turn translates it into meaningful data for the service consumer.

As traditional voice service revenues continue to shrink, mobile network operators are increasingly interested in MTC-based applications to bridge in the growing revenue gap [7]. Consequently, European Telecommunications Standards Institute (ETSI) has

started new activities with the goal of defining an end-to-end MTC architecture [8], whereas emerging Institute of Electrical and Electronics Engineers (IEEE) 802.16p proposals address enhancements for IEEE 802.16m technology to support MTC applications [9]. The recent analysis in [10] indicates that smart grid may become one of the key MTC use cases that involves meters autonomously reporting usage and alarm information to grid infrastructure to help reduce operational cost, as well as to regulate a customer's utility use based on load-dependent pricing signals received from the grid [11].

We expect that cellular technologies, such as Third Generation Partnership Project (3GPP) LTE and IEEE 802.16, will play a pivotal role in enabling smart metering applications. 3GPP LTE has recently defined several work items on MTC communications, primarily with respect to Radio Access Network (RAN) overload control [12; 13]. The 3GPP Services group is also interested in MTC-related improvements for LTE Release 12 within the context of mobile data applications [14].

Summarizing the latest developments in 3GPP, ubiquitous smart grid deployments were shown to be hindered by many technical challenges. In this Thesis, we consider a typical smart metering MTC application scenario in 3GPP LTE-A wireless cellular system featuring a large number of devices connecting to the network near-simultaneously and then sending their data through the network. We target thorough simulations and analysis of the Physical Random Access Channel (PRACH) within the LTE-A technology with respect to the congested MTC scenario and discuss some related research in what follows.

1.3 Related literature

Thorough evaluation of PRACH capacity, both with simulations and analytically, has been a popular research direction around 10 years ago for the legacy 3rd Generation (3G) cellular networks based on Code Division Multiple Access (CDMA) technology [15]. Originally, PRACH served as an Uplink (UL) contention-based channel to carry control information from client devices to the base station [16].

More specifically, a transmission of a random access request from a network client has been decomposed into two stages. At the preamble transmission stage, the power ramping technique was used to adjust the transmit power to particular channel conditions (see the related analysis with respect to the blocking, throughput, and delay in [17]). The basic principle of the power ramping procedure is that a user starts sending its preambles with lower power and then gradually increases its transmit power in case a transmission failed at the previous attempt. As a result, less interference is caused to other network nodes and actual data transmission begins with already adjusted power. Further, a meaningful message was transmitted to the base station for the purposes of initial network access or bandwidth requesting.

The improved version of PRACH within the 4th generation (4G) LTE-A system has

also attracted significant research attention. Considering a superior Orthogonal Frequency Division Multiple Access (OFDMA) technology, the successful transmission probability and throughput of PRACH were studied in [18]. An alternative approach to the throughput and access delay evaluation of PRACH has been pursued in [19] also providing several options for enhanced PRACH resource utilization.

Importantly, all the aforementioned research efforts have only considered the lighter loads from human-oriented traffic and thus the related results are not directly applicable to MTC scenarios where a large population of devices attempts to access the network within a very short period of time.

Accounting for a surge in initial network entry, many recent works focus on overloaded PRACH performance. Reflecting some initial discussions in 3GPP identifying the key impact of RAN overload, the work in [20] reviewed potential solutions and technology options to enhance the capability of LTE-A to handle numerous requests from MTC devices. Alternatively, [21] compared the two most probable (as per ongoing 3GPP discussions) candidate solutions for random access preamble allocation and management.

However, previous work on RAN overload has rather been a set of candidate proposals while 3GPP was evaluating those identifying the minimal required changes to LTE-A specification. Most recently, the research in [22] concludes on some of these efforts by detailing the officially approved 3GPP evaluation methodology produced within the work item on RAN overload control [23].

Summarizing, the existing frameworks for PRACH evaluation are mostly simulation-based. Furthermore, the obtained simulation results are often disjoint and even contradictory due to the lack of a unified methodology. As long as the recent calibration data approved by 3GPP has not been accounted for, many older findings may not be trustworthy for the community anymore.

In this Thesis, we develop a novel PRACH evaluation methodology building upon the calibrated baseline and conduct thorough analysis and simulations of the PRACH performance under MTC overload. We also give our prediction for the regular MTC operation, when the network is not experiencing a congestion.

Due to the fact that the MTC devices are typically small-scale and battery-powered, accounting for their energy consumption is of paramount importance [11]. In what follows, we seek to extend a validated evaluation methodology fully compatible with the 3GPP test cases with an in-depth analysis of PRACH performance in overloaded MTC scenarios. By including energy consumption into our framework together with the traditional performance metrics (such as access delay and success probability), we aim at providing a complete and harmonized insight into MTC device operation.

2. TECHNOLOGY BACKGROUND

This Chapter is related to the LTE-A, which is considered as technology candidate for future MTC deployments. The MTC concept is first described in more details. After that, basic properties of LTE-A, as well as the description of its access channels are given. Emphasis of the Chapter is made on the weaknesses of a main control channel used in the system under MTC conditions. Furthermore, possible alternative is introduced and analyzed.

2.1 MTC concept

MTC may be defined as information exchange between a *device* and another entity in the Internet or the core network, or between the devices themselves, which does not require human interaction. As such, MTC is a very distinct capability that enables the implementation of the *Internet of Things* (IoT). The mobile network operators are increasingly interested in the IoT applications to bridge in the growing revenue gap, as Average Revenue Per Unit (ARPU) of traditional services continues to shrink.

Due to its huge market potential, cellular technologies are currently developing air interface enhancements to support the IoT. In particular, 3GPP is becoming increasingly active in this area with several work items defined on MTC, especially for LTE-A Release 12 [14]. A conceptual draft of the MTC network, based on the LTE-A deployment is shown in Figure 2.1

Related research in [24] suggests that a service optimized for MTC is expected to be considerably different from that for conventional Human-to-Human (H2H) communications. This is particularly true for *smart metering* applications autonomously reporting usage and alarm information to grid infrastructure [11]. For instance, a potentially very large number of unattended meters, with little traffic per device, may introduce a surge at the serving base station when accessing the network nearly simultaneously [23].

The motivating smart metering use case therefore serves as a valuable reference MTC scenario [25] covering many characterizing MTC features. Together with effective measures for overload control in smart grid, the LTE-A system shall also provide mechanisms to lower power consumption of small-scale battery-powered wireless meters. As transmitted data bursts may be extremely small in size, the network should additionally support efficient transmission of such packets with very low overhead.

Accounting for the fact that MTC transmissions may be infrequent with large amounts

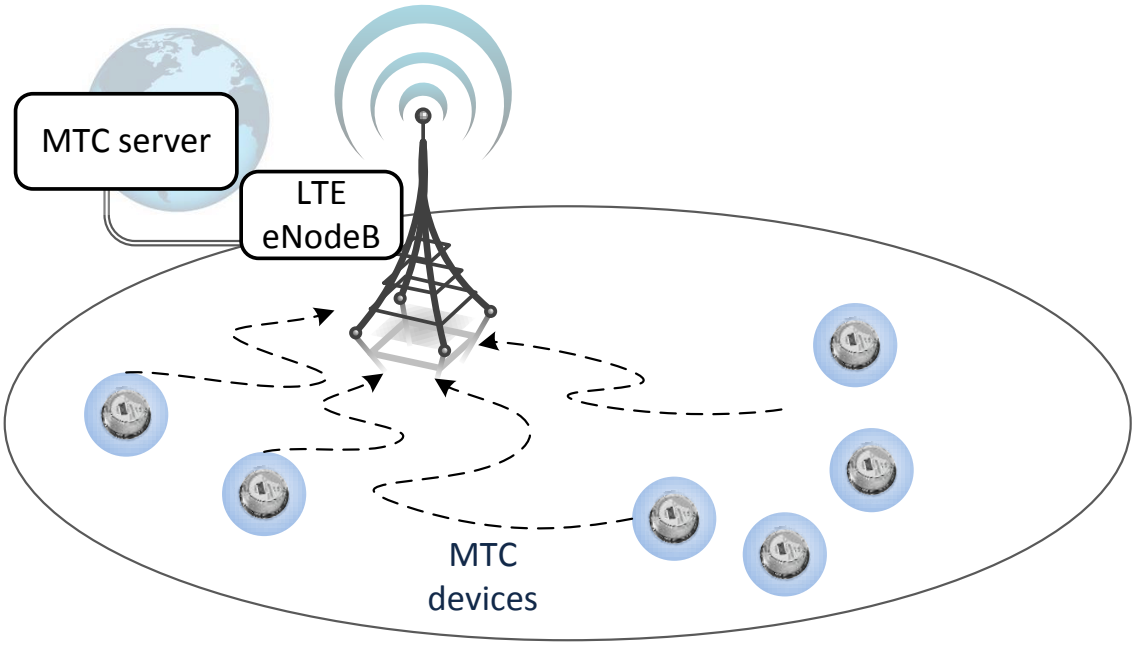

Figure 2.1: MTC network system topology.

of time between them, in this Thesis we target efficient support for small data access within the 3GPP LTE-A system. Also we emphasize that MTC devices should consume very low operational power over long periods of time and address energy-related performance across our study. We note that these important research problems are insufficiently highlighted in the existing literature which has only been focusing on overload control.

2.2 LTE-A components and structure overview

3GPP LTE-A is a cellular-based wireless network belonging to the 4th generation (4G), which development is ongoing for at least last six years. The main advantages of LTE-A are better flexibility and higher data rates. However, these features come with higher protocol complexity and more advanced techniques applied primarily at the physical layer. Below we briefly mention the basics of LTE-A topology and some physical layer features.

The architecture of an LTE-A network consists of two major components: evolved Universal Mobile Telecommunications System (UMTS) Terrestrial Radio Access Network (EUTRAN) and Evolved Packet Core (EPC) [26]. The main elements of EUTRAN are User Equipment (UE) and Evolved Node B (eNodeB). In this Thesis, we are mostly concentrated on the EUTRAN part (see Figure 2.2), specifically, on the connections between UE and eNodeB. Particularly, we focus on Frequency Division Duplex (FDD), which means that we are considering the frame type 1 [27]. Currently, the LTE-A system defines the smallest physical resource element and, depending on the configuration, 72 or 84 of them are combined into a single Resource Block (RB). In the UL, one RB includes 12 subcarriers in the frequency domain and 6 or 7 Single Carrier-Frequency Division

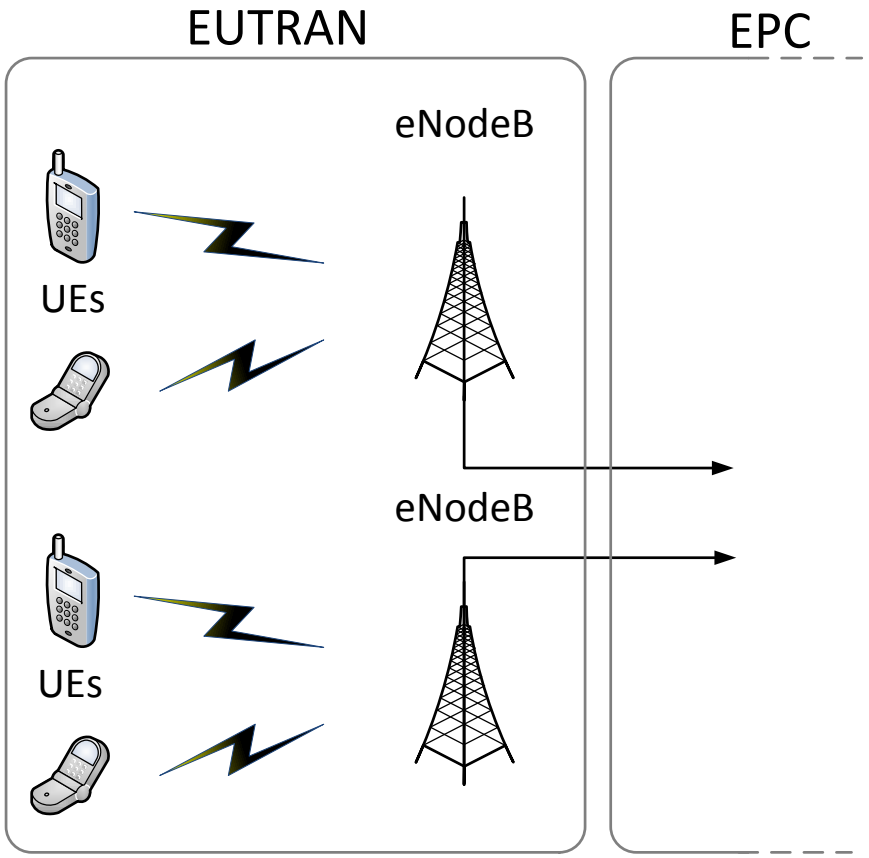

Figure 2.2: Simplified LTE-A EUTRAN architecture.

Multiple Access (SC-FDMA) symbols in the time domain [27].

One important feature of the physical layer is modulation and coding schemes (MCS). Changed radio environment causes variations in the Signal to Interference plus Noise Ratio (SINR) levels meaning that technology should support adaptation mechanisms to mitigate these fluctuations. Decreasing its MCS, the UE reduces the coding rate such that the SINR level needed for the successful data reception is also reduced by sacrificing maximum system throughput. There are 32 MCS sets as per LTE-A release 10 [28] and if adaptive MCS is enabled it can automatically adjust performance to the varying channel conditions.

In this research, we limit our investigation to a popular configuration of 5 MHz bandwidth with 25 RBs in frequency (see Figure 2.3). In the time domain, an RB is 0.5 ms in length, while an RB-pair (2 adjacent RBs) is forming a subframe of 1 ms and is the smallest schedulable unit. Ten subframes compose a radio frame of 10 ms. In Figure 2.3, the frame resources are split between the three channels: Physical Uplink Control Channel (PUCCH), PRACH and Physical Uplink Shared Channel (PUSCH). While PUSCH is usually used for useful data transmission, the other two are dedicated for control purposes.

To understand the signaling problems that could occur in LTE-A under MTC conditions in next subsection we will make a short overview of these two channels.

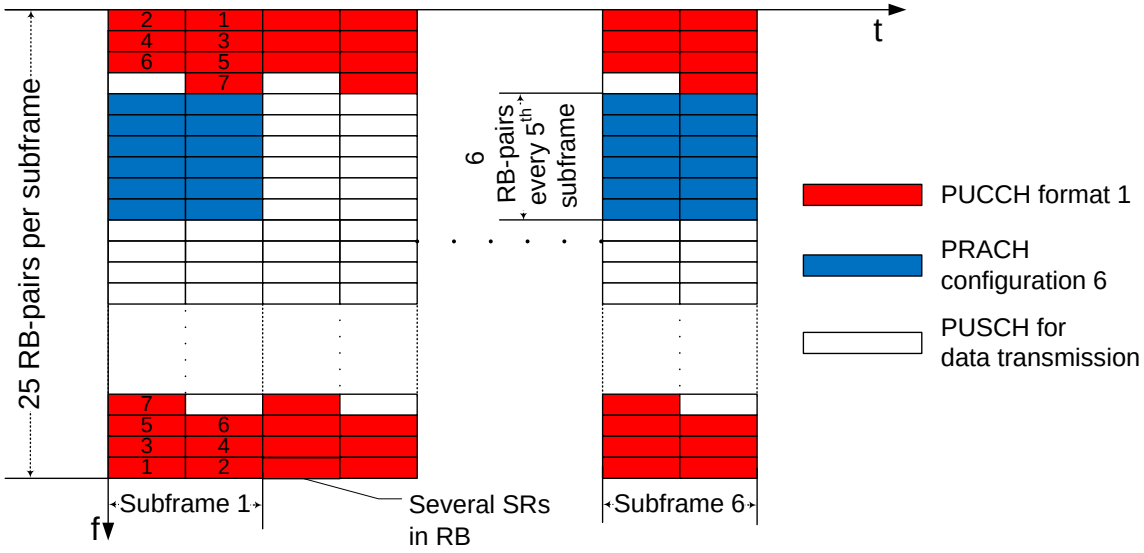

Figure 2.3: Distribution of resource blocks across data access channels.

2.3 LTE-A access channels

2.3.1 PUCCH

Description

PUCCH is dedicated to carry the UL control information including (i) channel quality information for adaptive control of modulation and coding schemes (MCSs) and power, (ii) Scheduling Requests (SRs) to demand system resources, (iii) indicators for MIMO control, and (iv) Hybrid Automatic Repeat reQuests (HARQ) feedback. Out of several PUCCH configurations, we are only interested in type 1 PUCCH RBs used for SR transmission (see Figure 2.4, left).

Problems in MTC environment

The default mechanism to allocate a part of PUSCH resource for UL data transmission is based on SR transmission. In case a device already has UL time alignment and a dedicated PUCCH allocation, it may use this allocation for sending its SR (see Figure 2.4, left), otherwise, PRACH will be used (see Figure 2.4, right). The periodicity of PUCCH RB availability for the SR transmission depends on SR configuration index and may vary from 1 to 80 ms (subframes). Moreover, several SRs from different devices can be aggregated into a single PUCCH RB and in our research we assume that up to 18 requests may be multiplexed [29].

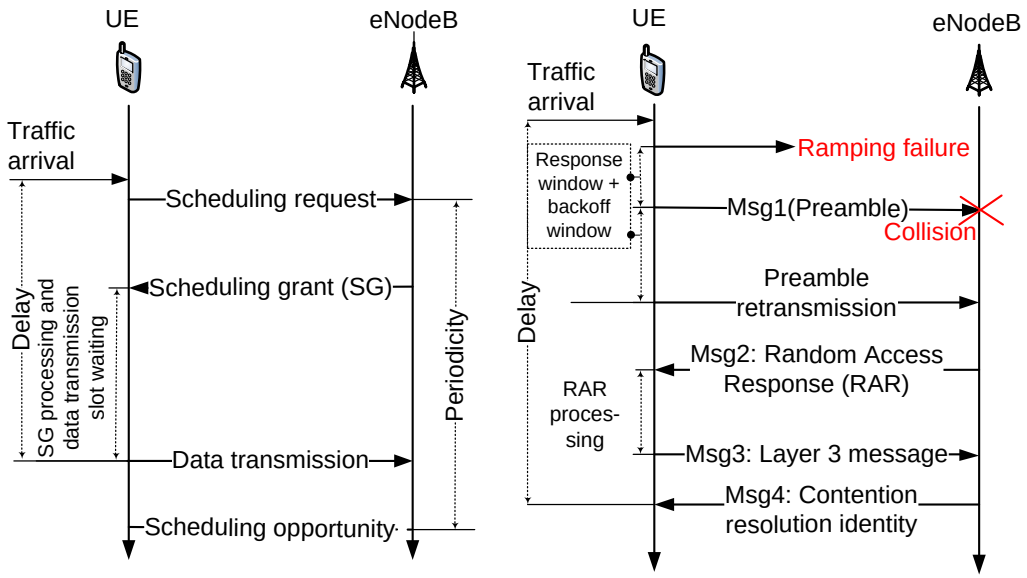

Figure 2.4: PUCCH (left) and PRACH (right) example signaling.

After sending its SR, the device needs to wait until the eNodeB (base station) answers it with a corresponding scheduling grant (see Figure 2.4, left and Figure 2.5). The main benefit of the SR transmission via PUCCH is very high reliability and nearly deterministic data delay values. However, when the number of devices is large, the PUCCH resources may quickly exhausted.

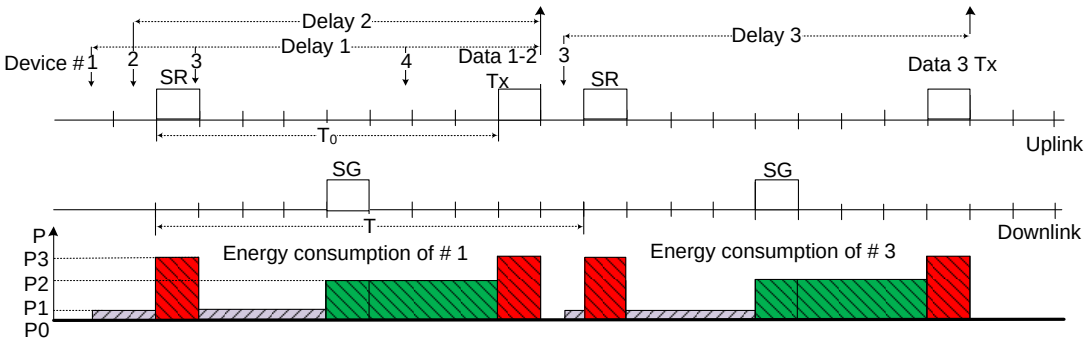

Figure 2.5: Example PUCCH time diagram.

When the PUCCH resource becomes insufficient to support every active device in a particular cell, another RB pair can be allocated or SR periodicity may be increased. In either case, SR transmission via PUCCH is expected to consume much system resources when the device population is growing. In the extreme, the PUCCH resources may become depleted even for longer periods and higher RB multiplexing orders. As mentioned earlier, an alternative method for SR transmission is the Random Access (RA) procedure over the PRACH.

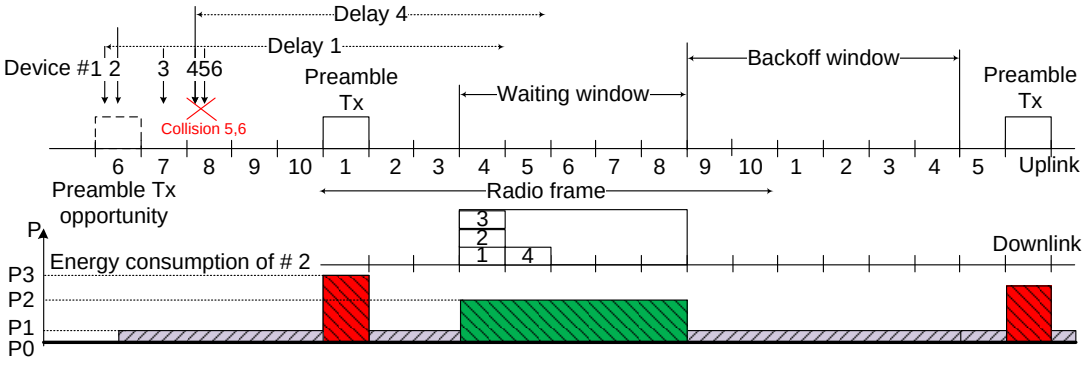

Figure 2.6: Example RA time diagram

2.3.2 PRACH

Description

RA procedure of 3GPP LTE-A is briefly summarized in Figure 2.4(right). Firstly, a UE sends a random access preamble (Msg 1) to the base station via the PRACH by choosing it randomly out of the maximum of 64 preamble sequences [30]. Note that fewer preambles may actually be available, depending on the network configuration. A collision can occur at the base station when two or more UEs choose identical preamble sequences and send them at the same time. Preamble transmission may also fail due to insufficient transmission power.

If a preamble has been received correctly, the base station (eNodeB) acknowledges it by a Random Access Response (RAR or Msg 2) within the response window. An indicator of the resource in Physical Downlink Shared Channel (PDSCH) where RAR can be received is sent over Physical Downlink Control Channel (PDCCH) [31].

As eNodeB needs to establish which UE sent which preamble, collision resolution process is required. After some RAR processing time, UE transmits Radio Resource Control (RRC) connection request message (Msg 3) via the PUSCH using the resources granted by Msg 2. RA procedure ends with a successful reception of RRC connection set-up message (Msg 4) from eNodeB. When more than one UEs send a similar Msg 3 (due to a preceding preamble collision), eNodeB will at best respond only to one of these requests. Otherwise, if any of signaling messages has not been received by UE, it restarts the RA procedure after some backoff time chosen randomly within a window given by the Backoff Indicator (BI). In Figure 2.6 the procedure is shown in more details including power consumption, which will be described later on.

Problems in MTC environment

By contrast to PUCCH, the PRACH transmission is unreliable and may be unsuccessful not only when sending Msg1 (due to collision or insufficient transmit power), but also due

to problems in the transmission or reception of the later messages required to finalize the procedure. All failures during the RA procedure lead to restarting it after a random time. Upon a restart, the backoff timer is chosen uniformly within the backoff window size of 20 ms [23].

As a summary, several negative events may be the cause of a failed RA procedure and hence higher network access delays. Naturally, collision probability increases with the number of requesting UEs (or, in our case, MTC devices) and also depends on their traffic patterns. For overloaded PRACH scenarios, the number of contending devices per cell may reach the astonishing number of 30 000 [32], which may lead to prohibitive collision probabilities and quickly deteriorate system resources. Therefore, the 3GPP has recently been very active on evaluating the causes and consequences of such overloads.

Despite its limited reliability, the main advantage of the PRACH procedure is that it consumes a fixed amount of RBs. For example, one PRACH allocation may occupy exactly 6 RB-pairs per subframe (see Figure 2.3 and [23]) and the devices may attempt to transmit their preambles only in subframes 1 and 6. However, with the increasing number of devices or their traffic arrival frequencies, the collision probability may become high, as well as access delay and power consumption due to retransmissions. Additionally, the extensive use of PRACH for the data access may block other MTC or H2H users performing initial network entry. Therefore, below we propose an alternative data access scheme for MTC devices.

3. ASSESSMENT

In this Chapter we are briefly discussing 2 main approaches used in the Thesis: simulation and analysis. In first section we are concentrating on simulation approach, considering System-Level Simulator (SLS) tools as an example of practically used simulator types. Moreover, during this research, we made a comparison of so-called general-purpose and problem-oriented SLS tools by driving experiments of cellular network LTE-based scenarios. After that, we also consider the mathematical analysis of LTE-A PUCCH-based access method to show that analytical approach could be a useful and convenient tool to describe the modern wireless networks behavior.

3.1 Simulation paradigm and capabilities

3.1.1 SLS concept

Contemporary wireless communications are one of the most rapidly growing segments of the market. Novel solutions and features are being actively developed and deployed in this field. However, the analysis of modern wireless networks requires significant resources. To facilitate performance assessment, SLS tools are typically used. Their main purpose is to predict how the network will operate before actually running it in a real environment. This is very helpful, because network operator may lose a lot of resources if the proposed technology will not work properly after the network deployment. Moreover, system level simulators can be used as network planning tools and for educational purposes.

There exist different criteria to classify the available SLS tools: efficiency, complexity, scalability, etc. However, we may broadly divide them into two large classes: general-purpose and problem-oriented. Several examples of general-purpose SLS tools are shown in Table 3.1. It will be fair to say that the evaluations shown in Table 3.1 are based on the personal opinions and belief of the author. More information about the mentioned simulators can be extracted from the respective websites (see references in Table 3.1).

General-purpose solutions are wider than their problem-oriented counterparts and may include different technologies as so-called “modules“ inside one integral tool. The major disadvantage of the simulators belonging to this class is not very detailed (simplified) system structure. As the result, they are sometimes not enough accurate, or their performance cannot be verified. Another drawback is the complexity of their source code. General-purpose SLS tools are typically used for the educational purposes, that is, to study the

Table 3.1: General-purpose SLS examples

Name	Detalization	Usability	Complexity
Opnet modeler 17.0 [33]	High	High	High
OMNet++ [34]	Medium	High	High
NS2 [35]	Low	Medium	Low
NS3 [36]	Medium	High	Medium
GNS [37]	High	High	High
Hurricane 2 [38]	Low	Medium	High

basic principles behind a particular technology. They can also be applied in academic research [39], and Opnet modeler by OPNET Technologies is a typical representative within its class.

Problem-oriented SLS tools are specifically produced for the simulation of upcoming wireless technologies and are mainly developed by the network operators, vendors, or with the assistance of some third-party companies. Advantages of these simulators are: simplicity of usage, wider opportunities for calibration, and broader range of available statistics. However, the simulators belonging to this class are typically not intended for commercial use. The reason is that these SLS tools have smaller performance scope. They are normally exploited within companies for detailed research on specific technological issues and are therefore difficult to use in educational process. Particularly, problem-oriented SLS tools are important instruments exploited during the standardization process and the development of new technology.

In order to conclude on their precision, different simulators can be compared with each other and also against theoretical predictions. In particular, the most interesting statistics at the physical layer is related to throughput per user (or overall), spectral efficiency (center and cell-edge), SINR, and BLock Error Rate (BLER).

3.1.2 General-purpose and Problem-oriented SLS tools examples

Opnet Modeler

OPNET Modeler 17.0 [33] is a network simulator, which purpose generally is the modeling of different types of networks. The OPNET Modeler Wireless Suite presents plenty of capabilities and functions for various types of wireless networks including GSM, UMTS, IEEE 802.16 (WiMAX) and 3GPP LTE-A. Each network type is included as a separate module and is visible through graphical modules, called editors. The **Project Editor** defines the basic functionality of network planning. Every network element (node) in the Project Editor can be configured also in the **Node Editor**. Further, each block is represented as a finite state machine (FSM) that can be adjusted in the **Process Editor**. The

typical work flow to create a new model is demonstrated in Figure 3.1.

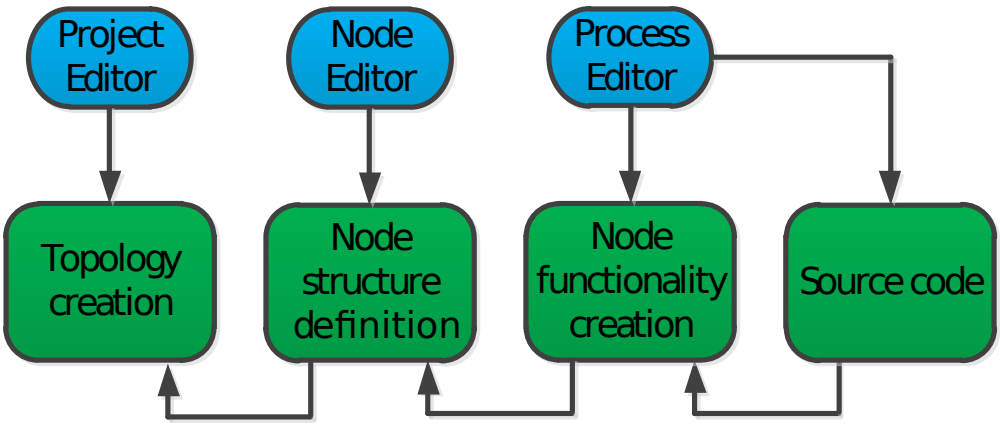

Figure 3.1: Model creation workflow in Opnet modeler.

Our module of interest is the LTE-A module, which includes different eNodeB models, UE models, and an EPC model. Moreover, it has a complex and wide structure with a number of limitations and parameters to configure. In the scope of this Chapter, the most important component of the LTE-A module is the **Physical Layer Measurements**. It includes SINR measurement in both Downlink (DL) and UL directions, which are collected separately for each UE.

Other interesting statistics at the physical layer is related to the Reference Signal Received Power (RSRP) and reference signal received quality (RSRQ). A UE measures RSRP and RSRQ continuously (with a 5ms update interval) and independently for each eNodeB, which it can hear. Continuing with physical layer measurements, we should also mention **Pathloss, Interference**, and **Multipath Fading** models supported by the module. For instance, the following pathloss models are available in the Opnet modeler [33]: Macrocell suburban based on COST231 Hata Urban model, Macrocell urban based on COST231 Hata Urban model, Microcell urban based on COST231 Walfish-Ikegami, Erceg suburban fixed, and shadow fading based on the lognormal distribution model. Speaking about multipath propagation, four International Telecommunication Union (ITU) multipath models are supported [33]: Pedestrian A and B, as well as Vehicular A and B. Finally, the interference model is supported as follows [33]:

- Interference module detects time and frequency overlaps among different bursts.
- Interference is proportional to the amount of burst overlaps.
- Interference may cause burst drops for PUSCH and PDSCH bursts.

- Interference effects for control channels are based on a probability distribution function.

- Interference is computed among nodes using the same or different LTE-A physical layer profiles.

- The frequency attributes of a given LTE-A physical layer profile are accounted for when computing interference.

UNN LTE UL SLS

The UNN LTE UL SLS is an example of a problem-oriented SLS mentioned above and designed primarily to assess client cooperation techniques in mobile networks. Additionally, it allows for the evaluation of the advanced data transmission techniques. This SLS has been developed by the Wireless Competence Center (WCC) of the State University of Nizhny Novgorod and is based on the SLS used by Russian Evaluation Group within the International Mobile Telecommunications-Advanced (IMT-Advanced) standardization process intended for the evaluation of LTE-A as a 4th generation system candidate [40].

In contrast to the general-purpose SLS tools, the UNN LTE UL SLS has no support for higher-layer algorithms. Further, it has a simplified interface, flexible configuration tools, and convenient post-processing instruments. However, the major feature of the UNN LTE UL SLS is the possibility of detailed and accurate simulations of the technology in question and of the deployment scenario including layout, antenna configurations, and channel models.

The UNN LTE UL SLS supports simulation methodology typical for problem-oriented SLS tools and is actively used by the international standardization committees (e.g. 3GPP, IEEE, ITU, etc.), as well as equipment manufacturers. Particularly, hexagonal layout is assumed with base stations located in the centers of hexagonal cells and with UE uniformly and randomly distributed over the entire simulated area. Each base station has 3 sectors divided by different sectors antenna beams. Further, the eNodeB entities located in each sector perform power control, scheduling and resource management for the associated UE similarly to the real-world algorithms operated at the currently deployed base stations. Data packets are transmitted from UE to eNodeB and the success of each packet reception is modeled depending on the physical layer algorithms operation and signal propagation conditions: transmit power, path loss, channel models, interference from other transmitting UEs, etc. Then, system operation statistics is stored and analyzed further to derive the required SLS results.

The UNN LTE UL SLS structure is provided in Figure 3.2. The simulator has been developed within the framework of the common SLS platform. The basic principle of

common platform is the division of SLS functionality into two main blocks: system-independent part which is fully reusable between different problem-oriented SLS tools for different mobile radio-access networks or for different purposes, whereas system-dependent part is developed specifically for the system under consideration. The interface between system-independent and system-dependent parts is formalized and minimized to simplify porting of system-dependent part between different simulators.

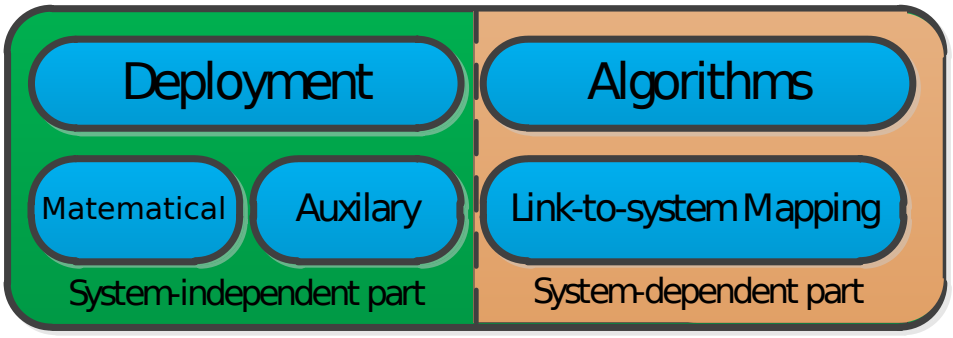

Figure 3.2: Key components of the UNN LTE UL SLS

Along with the auxiliary functionality, the system-independent part includes the deployment module responsible for the simulation of layout, antenna models, channel models, etc. and its own mathematical library optimized for and oriented at SLS purposes. System-dependent part was developed directly for the LTE-A Release 10 UL and in turn consists of two program modules: Link-to-System (L2S) mapping interface and implementation of the main system control algorithms. L2S mapping interface is used for fast and accurate prediction of the packet transmission performance of each link avoiding the exact direct modeling of physical layer processing in the system. Simulated system control algorithms include power control and scheduling, mentioned above, and HARQ algorithm.

At the beginning of this research, the basic functionality of the UNN LTE UL SLS is designed and implemented, whereas further development is also considered. In particular, there is a large field for considered problem-related improvements of the SLS. Enhancements of the program platform are also planned, primarily with respect to input (configuration) and output (Simulation Results Analyzer) tools.

3.1.3 SLS tools comparison

Parameters

In this work we are firstly comparing both simulators on a small-scale simplified scenario that can be also evaluated theoretically. This ensures that both SLS tools give adequate and predictable results. Further, we consider scenarios with more advanced physical effects and evaluate the difference in performance by both tools.

Basically, some mismatch is expected due to the difference in signal power distribution dependent on the antenna pattern representation. Both simulators have flexible 3-D antenna pattern editors, which allow setting basic antenna parameters. As UE antenna is omni-directional, the core difference is in the BS antenna representation. The main antenna parameters are explained in Figure 3.3. All these parameters are configured for both simulators and have a significant impact on the network performance. Antenna gain here is a gain in transmitted/received power, because of antenna directivity (in comparison with non-directional antenna. Half power beam width (HPBW) is an angle, which shows where the gain of the antenna decreases on 3dB. Antenna downtilting is an angle of antenna tilting. Its purpose is to create a proper BS coverage. And forward to back ratio is a ratio between antenna gain in main direction ant its opposite side.

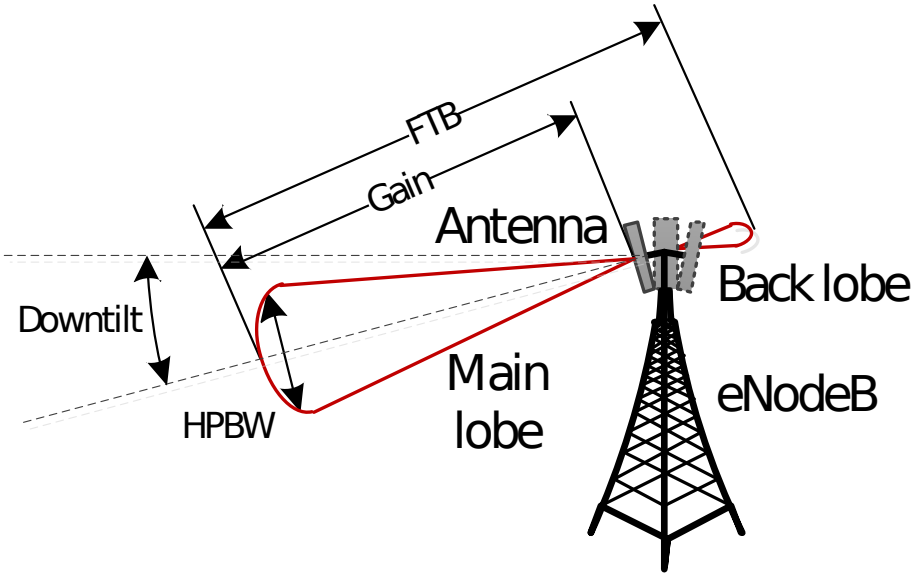

Figure 3.3: BS antenna parameters

The second difference may be due to the interference representation. If both power control and adaptive MCS are disabled, interference representation differences will become more evident. Opnet is expected to show higher overall throughput, whereas UNN LTE UL SLS should give lower numbers due to wrap-around. Technically, wrap-around carries the signals of border cells (as shown in Figure 3.4) into an opposite-side cell,

thus border cells do not have any advantage in interference environment comparing to the center cells.

This technique show more realistic results and gives calculation time economy in 19-cell scenario, because it gives us possibility to take into account not only a central cluster, as it shown in right side of a Fig. 3.4), but also border cells.

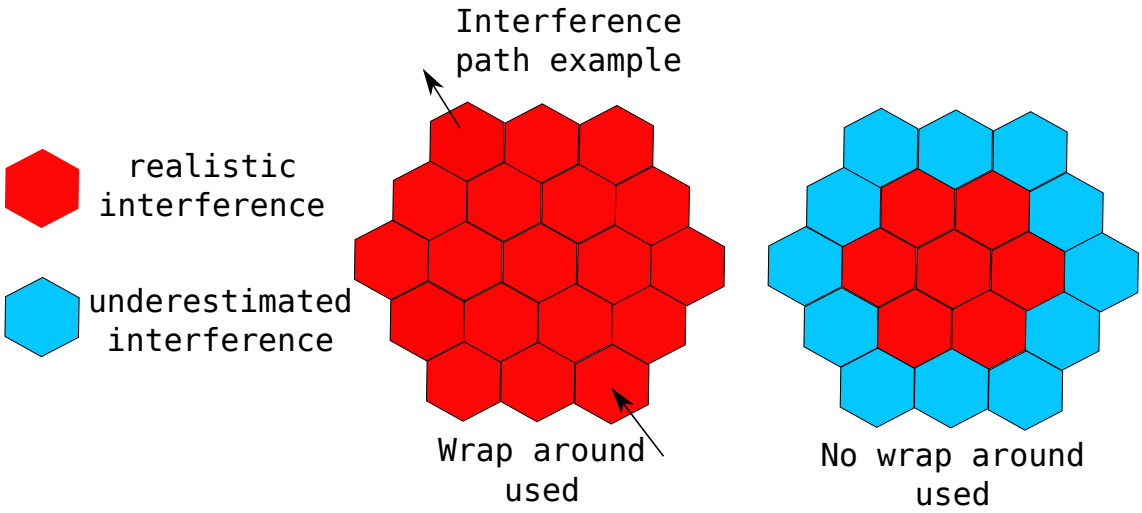

Figure 3.4: Wrap around signal path example (left side) and realistic interference zone without wrap around (right side) in typical 19-cell scenario

In this Thesis three scenarios are considered. Firstly, there is one-cell scenario with minimal physical effects. The purpose of this scenario is to compare both SLS tools against the theoretical predictions. Secondly, there is one-cell scenario with complete physical layer effects in order to highlight the difference between the SLS tools on a smaller scale. Thirdly, there is a typical 19-cells scenario, which is capturing the interference effects. Baseline parameters for all the three scenarios are summarized in the Table 3.2. Also some assumptions can be made for simplicity:

Assumption 1. No HARQ.

Assumption 2. No sounding reference signals (SRS).

Assumption 3. No link adaptation and no channel-dependent scheduling.

Assumption 4. No penetration losses.

Assumption 5. The locations of users are chosen in a random fashion.

Also, some overhead is known to be presented in Opnet due to the explicit modeling of the control channels. Therefore, it should be taken into account in UNN SLS and

Table 3.2: Baseline simulation parameters

Parameter	Value
Inter-cell distance	500 m (288 m cell radius)
Number of users per cell	30 users per 3-sector cell (10 users per sector)
UE antenna configuration	omni-directional, antenna gain 0 dBi
BS antenna configuration	directional, 17 dB in boresight gain
BS antenna HPBW	azimuth plane = 70 deg, polar plane = 15
BS antenna downtilting	12 deg
BS antenna FTB	20 dB
Number of BS and MS antennae	1
MCS	7, 14, 21
Used bandwidth	10 MHz (1 MHz guard band)
Base frequency	1920 MHz
Used mode	FDD
Cyclic prefix	Normal
Scheduler type	Round-Robin scheduler (FDS)

in theoretical results. Basically, there is PRACH that takes 6 resource block pairs in one subframe out of 10 (each frame), decreasing the throughput by around 1.2 % on average (0.988 in (3.1)), and PUCCH, that takes 1 additional resource block pair in each subframe. In Opnet modeler, Frequency Division Scheduling (FDS) is used meaning that resource blocks are equally divided between all the users in a sector. For this case, there exists a simplified method to calculate the physical-layer throughput. One should take a Transport Block Size (TBS) value for a given number of RB (Table 7.1.7.2.1-1 in [40]) and divide it by the length of the subframe (3.1) to obtain the throughput of one user. If there are 10 users in the cell, Opnet will allocate 5 RB for 9 of them and 4 RB for the last one. Therefore, the calculations must be presented for each of the 10 users separately. Summarizing, the theoretical throughput for one user can be defined as:

$$T = t \cdot 0.988/m, \tag{3.1}$$

where t is the TBS value, T is the theoretical value of the throughput, and m is the subframe length.

Scenarios

One-cell with minimal physical effects. For verification purposes, one hexagonal cell with 3 sectors and 10 users in each sector was considered. The limitations for this scenario are: no mobility (all users are static), no multipath, and no shadow fading. The related parameters are given in Table 3.3.

Table 3.3: Simulation parameters-I

Parameter	Value
Transmission power, per RB (per UE)	23 dBm
Transmission power, overall (per UE)	40 dBm
Path loss model	Free space

One-cell with complete physical effects. This scenario is similar to the previous one, but physical effects are taken into account and the system is not anymore static. The parameters for this scenario are shown in Table 3.4.

Table 3.4: Simulation parameters-II

Parameter	Value
Transmission power, per RB (per UE)	13 dBm
Transmission power, overall (per UE)	30 dBm
Path loss model	3GPP 25.996 Urban macrocell
Multipath model	ITU pedestrian A
User speed	3 km/h

19-cells scenario. The third scenario is a typical 19-cells setup (see Figure 3.5) [40]. In each cell, there are 3 sectors and 10 users per sector. Hence, the total number of users per a simulation run is 570. The parameters are effectively the same as before, but the interference is accounted for explicitly.

Results

Equation (3.1) was established for 1 user per sector. However, in case of 10 UE per sector, each of them has 5 RB per subframe on average. As such, the overall throughput is 16.978 Mbps per cell. Theoretical throughput for one user, with parameters defined in Subsection 3.1.3 is shown in Table 3.5.

Table 3.5: Theoretical throughput for ideal channel conditions

MCS	7	14	21
Average throughput per UE, Mbps	0.565	1.215	2.085
Overall throughput, Mbps	16.978	36.469	62.552

In Tables 3.6, 3.7, 3.8, and in Figures 3.6, 3.7, 3.8 the values of throughput for all the three scenarios are shown. In the first scenario, one may see that the throughput is lower than theoretical for both SLS tools, whereas Opnet modeler demonstrates more optimistic results. Dramatic reduction of throughput in case of MCS=21 can be explained

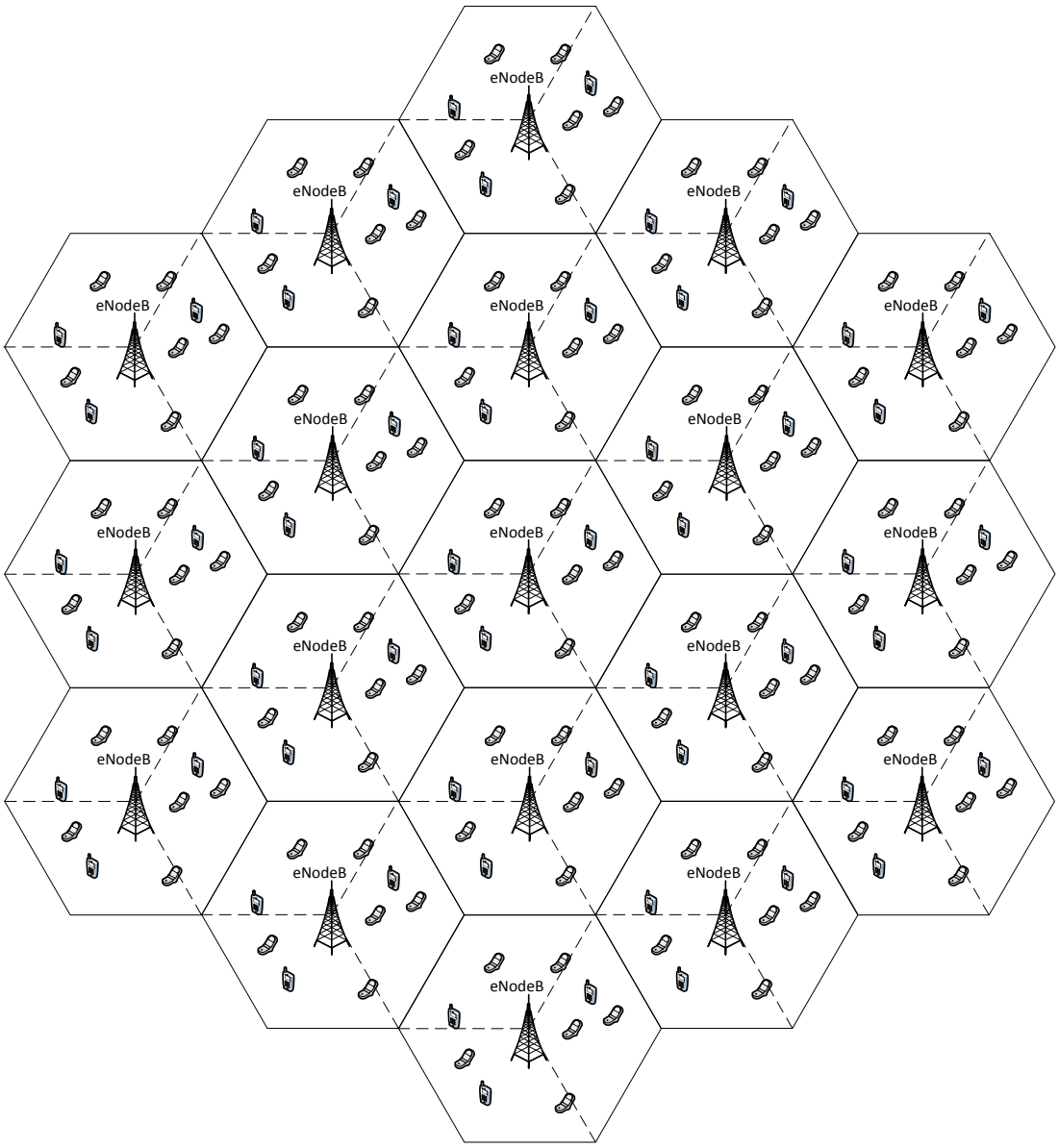

Figure 3.5: 19 cells deployment example

by the higher BLER values for cell-edge (sector-edge) users. Typically this occurs with a cell/sector-edge users, because they have a highest path loss and lowest SINR and then MCS becomes higher, BLER also grows.

Theoretical values can be achieved by accumulating the throughput and the traffic that was lost due to increased BLER. In equation (3.2), it is shown how to calculate loss S, where T is the initial throughout, B = BLER, and G = 1-BLER.

$$S = (T \cdot B)/G \tag{3.2}$$

For example, in case of MCS=21 (first scenario) UNN LTE UL SLS gives the average

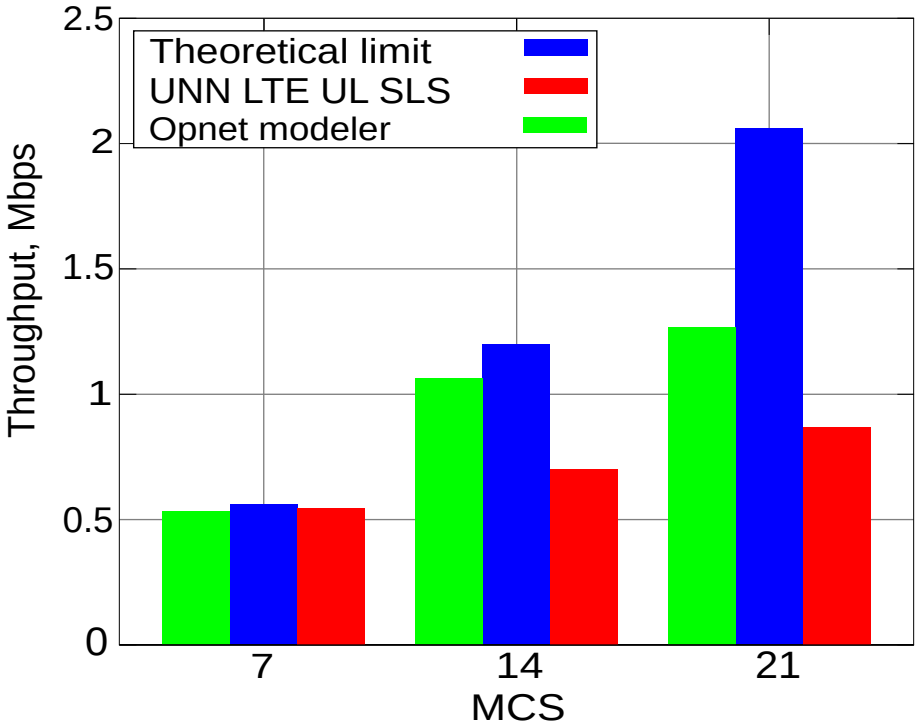

Figure 3.6: Average throughput per user, scenario 1

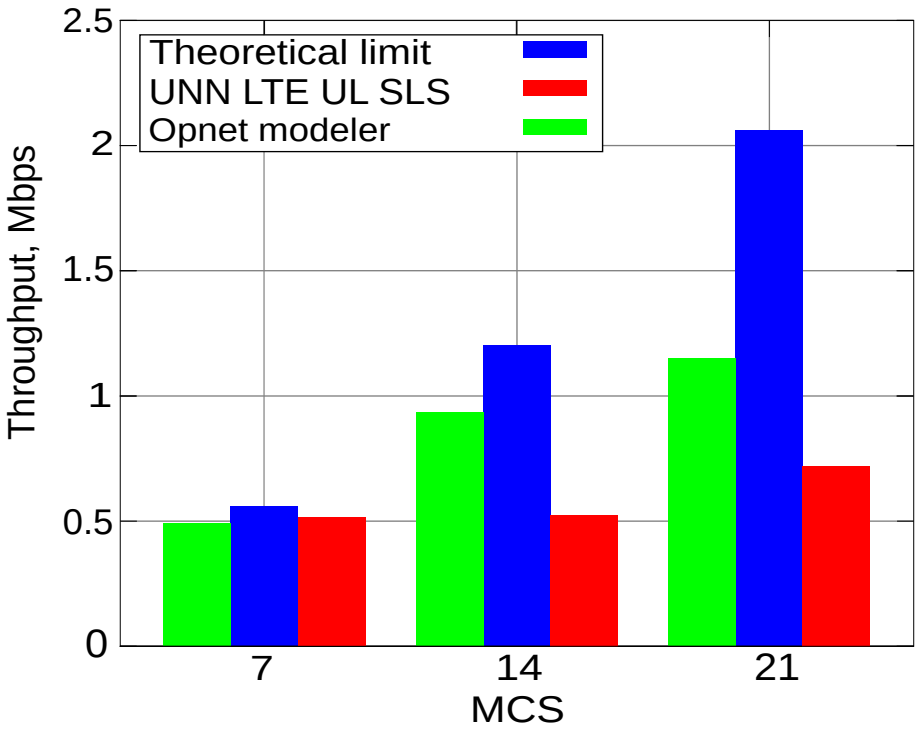

Figure 3.7: Average throughput per user, scenario 2

throughput of 0.88 Mbps, and the BLER is equal to 0.57. We thus can add 1.166 (according to the equation (3.2)).The sum is equal to 2.0465 Mbps, which is pretty close to the

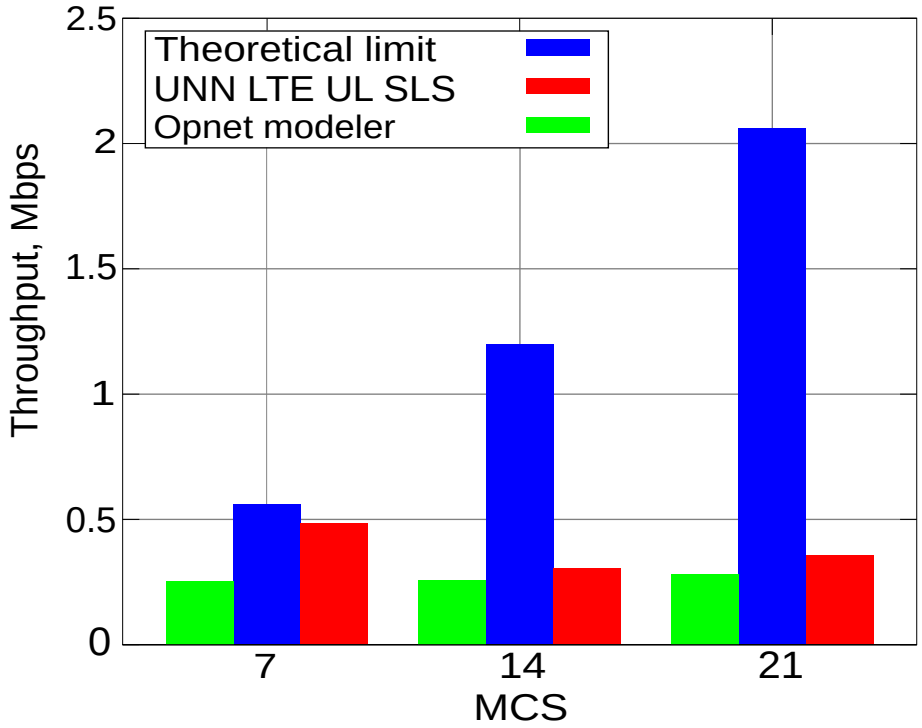

Figure 3.8: Average throughput per user, scenario 3

analytical result. Some difference, of course, still occurs due to probability of unequal drop within the cell. E.g. it can be so that in one sector there will be 11 users, and in a neighbor one 9. As a drawback these UEs will have different TBS.

Table 3.6: 1st scenario results

MCS	**7**	**14**	**21**
Opnet Modeler average throughput	0.533	1.063	1.266
Opnet Modeler average BLER	0.058	0.128	0.401
UNN LTE UL SLS average throughput	0.543	0.701	0.869
UNN LTE UL SLS average BLER	0.033	0.420	0.570
Throughput difference (%)	1.841	34.055	31.359

Our simulations showed that both SLS tools are close to the theoretical calculations, when MCS = 7 in first two scenarios. However, some mismatch occurs for higher MCS, which is explained by the growing BLER for users at the cell edges. Further performance differences between the SLS tools may be caused by unequal number of users associated (dropped) to (within) a sector and different interference representation in the first two scenarios. For the third scenario, we expected higher results for Opnet. However, Opnet modeler traffic generator works at the application layer, while UNN LTE UL SLS physical layer is always in the full-buffer mode. Thus, buffer may not always be full for Opnet

Table 3.7: 2nd scenario results

MCS	**7**	**14**	**21**
Opnet Modeler average throughput	0.366	0.55	0.733
Opnet Modeler average BLER	0.370	0.557	0.651
UNN LTE UL SLS average throughput	0.513	0.523	0.721
UNN LTE UL SLS average BLER	0.110	0.570	0.650
Throughput difference (%)	28.655	6.727	1.637

Table 3.8: 3rd scenario results

MCS	**7**	**14**	**21**
Opnet Modeler average throughput	0.252	0.257	0.280
Opnet Modeler average BLER	0.561	0.789	0.867
UNN LTE UL SLS average throughput	0.484	0.306	0.355
UNN LTE UL SLS average BLER	0.160	0.750	0.830
Throughput difference (%)	47.934	16.013	21.127

modeler. Additionally, UE movement is modeled explicitly in Opnet, whereas in UNN SLS only the UE channel deviations are accounted for.

Considering the above factors, we conclude that the results are theoretically predictable for both SLS tools and that the tools themselves match with a reasonable degree of accuracy given their limitations. Nevertheless, we may already conclude that Opnet performance is good enough for less detailed research at higher layers. However, it was observed that Opnet modeler is too slow and complicated to work with MTC scenarios, while UNN LTE UL SLS has not enough capabilities to simulate the PRACH in details. As a conclusion to the section we could say that for the purposes of this research a simplified (in terms of physical layer) Protocol-Level Simulator (PLS) was written, based on the principles of problem-oriented SLS tool, which will be in details described in the next Chapter.

3.2 Analytical benchmarking and limitations

3.2.1 General remarks

The below analysis of the two data access schemes has been conducted with two different approaches. Whereas the evaluation of the PUCCH-based mechanism is close to trivial, the analysis of the contention-based scheme (PRACH) is much more challenging. Due to the inherent memory of the contention process, addressing it straightforwardly has not been successful before even for much simpler ALOHA protocols. As such, we had to

adopt the equivalent memoryless models for the scheme.

Owing to a large number of available preambles in PRACH, taking into account all the transitions between the system states is unnecessarily complicated. Therefore, we study the PRACH-based data access from the point of view of a particular backlogged MTC device and its contention behavior by abstracting away most transitions through averaging. The obtained approximation is generally suitable for the low system loads, as long as the collision probability remains sufficiently small.

In this section we are considering the example of PUCCH-based data access analysis, to show how powerful and simple the analytical approach could be, giving more difficult analysis of PRACH in the next Chapter.

3.2.2 PUCCH-based data access analysis example

The PUCCH-based transmission is not susceptible to collisions and does not include back-off periods. The data packet transmission time is assumed to take 1 subframe. We thus calculate the mean packet delay as follows:

$$E[\tau] = T/2 + T_0 + 1, \tag{3.3}$$

where T_0 is the PUCCH procedure duration (see Figure 2.5), T is the SR periodicity, and 1 stands for the transmission time.

To estimate the power consumption, we obtain the time fraction that a device spends in every state (see subsection 11.5 for more details):

$$q_1 = (T/2+3)\cdot\lambda, q_2 = (T_0-3)\cdot\lambda, q_3 = 2\cdot\lambda. \tag{3.4}$$

The total amount of energy spent by the device may thus be derived from the expressions above as follows:

$$\varepsilon = P_2 q_2 + P_3 q_3 + P_1 q_1 + P_0(1-q_3-q_2-q_1). \tag{3.5}$$

4. LTE-A PRACH PERFORMANCE UNDER MTC CONDITIONS

Core algorithms, properties, assumptions and limitations of the research are presented in this Chapter. Proposed analytical and simulation tools calibration process is also shown and described in here.

4.1 Basic system parameters, assumptions and targeted metrics

Some initial parameters and assumptions related to simulations of LTE-A RACH for MTC scenarios have been proposed in [23]. The motivation behind this document was to identify the parameters of a verification scenario, as well as to present calibration data providing a trustworthy baseline for various 3GPP member companies. As such, it is very important that existing PRACH-related simulation frameworks are harmonized with respect to the results therein. Table 4.1 reviews parameters from several simulation methodology documents [23; 41]. In particular, PRACH configuration index defines subframe numbers, where a UE can attempt preamble transmissions, as well as the preamble length. The mac-ContentionResolutionTimer is the maximum number of subframes the UE waits after Msg 3 transmission and before considering the RA procedure as failed. Other settings have mostly been explained in the Chapter 2, while some additional parameters (out of the methodology scope) will be detailed further on.

As it was already mentioned, a comprehensive evaluation methodology for LTE-A RA procedure has recently been sketched in [23]. The MAC layer parameters are borrowed from [30] and for the most part detail the RA procedure which was considered above. According to the proposed methodology, most PHY layer features are abstracted away to simplify performance evaluation. It is assumed that out of those, the power ramping procedure has the most impact on the metrics of interest. The ramping procedure is meant for power control and has been detailed in [28]. In [23], this procedure has been reduced to a simple function e^{-i} that defines the probability of failure.

Another important aspect of the methodology is the considered traffic patterns. The document [23] is focused on the overloaded scenarios, which could theoretically cause abnormal system loads, high collision probabilities, and prohibitive RA procedure delays. In fact, as our subsequent analysis shows, only traffic type 2 (beta distribution) is causing

Table 4.1: Core simulation parameters

	Parameter	**Value**
-	Cell bandwidth	5 MHz
-	PRACH Configuration Index	6
s	Total number of preambles	54
L_1	Max. number of preamble transmissions	10
-	Number of UL grants per RAR	3
-	Number of CCEs allocated for PDCCH	16
-	Number of CCEs per PDCCH	4
-	Ra-ResponseWindowSize	5 ms
-	mac-ContentionResolutionTimer	48 ms
W	Backoff Indicator	20 ms
π_3/π_4	Probability of successful delivery for Msg 3/Msg 4	0.9/0.9
L_3	Max. number of HARQ Tx for Msg 3 and Msg 4 (non-adaptive HARQ)	5
M	Number of MTC devices	5K, 10K, 30K
N	Number of available subframes for device activation	10K, 60K
t_0	Subframe size	1 ms
b	Periodicity of PRACH opportunities	5 ms
K	RAR response window	5 ms
K_1	Preamble transmission time	1 ms
K_0	Preamble processing time at eNodeB	2 ms
t_{pr}	Processing time before Msg 3 transmission	5 ms
t_{tx}	Time of transmission of Msg 3, waiting, and reception of Msg 4	6 ms
P_0	Power consumption in inactive state	0.0 mW
P_1	Power consumption in idle state	0.025 mW [42]
P_2	Power consumption of processing and Rx	50 mW [42]
P_3	Power consumption during Tx	50 mW [42]

actual overloads. This overloaded scenario, however, is difficult to evaluate analytically and we analyze it mostly based on the simulation results. Traffic type 1 scenario is used primarily for calibration purposes and, in contrast to the other one, could be approximated and verified with our analytical approach.

Moving forward, we continue with more detailed system assumptions. One cell of 3GPP LTE-A is considered featuring M identical MTC devices. A device randomly

chooses a subframe for its UL activation following the uniform distribution (traffic type 1) or beta distribution (traffic type 2) over $[1,N]$. A preamble, which takes 1 subframe to be sent, may be attempted for transmission at each b-th subframe, i.e. at slots 1, $b+1$, ..., $b \cdot i+1$, $i \in Z^+$.

Whenever activated, the MTC device is said to be backlogged until the completion of its RA procedure. Otherwise, the device is inactive. At subframes of service (when there is a PRACH opportunity), every backlogged MTC device chooses one of s preambles and sends it. According to [23], we assume a collision when two or more MTC devices select the same preamble, and all the collided preambles are considered failed (ignoring the power capture effect) after some service time. Otherwise, the preamble is successful with the probability $1-e^{-i}$ due to the power ramping, where i is the number of the transmission attempt [23]. The maximum allowed number of preamble transmission attempts is L_1.

If a transmission fails due to the collision or insufficient power, the MTC device uniformly selects a backoff counter within W. After 2 subframes of pausing, the response window of size K starts (see Figure 2.6). Within the response window, eNodeB sends RAR messages in the subframe uniformly distributed over $[1,K]$. If the MTC device does not receive RAR, the preamble transmission attempt is considered failed and the device backoffs.

When the MTC device receives RAR successfully, it starts processing Msg 3 for transmission during t_{pr}. Further, it sends Msg 3 and waits for $t_{tx}-1$ to receive Msg 4 (see Figure 2.4, right). Msg 3 and Msg 4 are delivered successfully with the probabilities π_3 and π_4 respectively. The maximum allowed number of Msg 3 transmission attempts is L_3.

Complementing the 3GPP methodology, which is already considering delay, collision probability, and the average number of preamble transmissions, we propose an extended analysis of energy-related metrics. In this Thesis, we also consider some overload control mechanisms and regular system operation conditions, which, in combination with a detailed analytical model, is intended to complete evaluation of LTE-A RACH in MTC scenarios.

4.2 Simulation approach

4.2.1 Simulator description

In what follows, we detail our advanced protocol-level simulator of RA procedure and the related improvements. For the purpose of conducting extensive evaluations, existing network simulation tools were considered to be either inadequately slow or lacking the necessary signaling support. As such, a novel simulator has been developed taking advantage of extensible modular structure for improved scalability. The benefit of our simulator is its flexibility in the choice of the parameters of interest, including number of devices, signaling timings, processing mechanisms, and system settings such as number

of preambles, backoff window size, etc.

More importantly, our simulation tool allows for simple integration of the extended components, such as overload control mechanisms and power consumption measurements. Finally, the software is supplied with flexible statistics collecting and processing functions while is able to evaluate various parameters of interest ranging from access latency/probability to fine-grained energy-related metrics. All the messages transmitted over the same channel are multiplexed and processed jointly with explicit modeling of collision behavior. The operation of PRACH accounts for all the necessary features discussed previously.

In Figure 4.1, the simplified structure of the simulator is captured. There are three core classes implemented in C++: traffic generator, UE, and eNodeB. Traffic generator has support for three basic patterns: Uniform, Poisson, and Beta, which are configured for all the UEs at the beginning of a simulation run. Full buffer (saturated) model is also available as a separate option. Each device has a dedicated traffic generator implementing the chosen traffic pattern.

The UE class is supporting operation related to Msg 1 and Msg 3 transmission, as well as Msg 2 and Msg 4 reception. Several supplementary functions, such as power ramping, are also maintained at the UE side. The eNodeB class is responsible for detection of Msg 1 failures due to a collision or insufficient transmission power. After the detection procedure, a decision on whether to send Msg 2 is made. More detailed scheme of system behavior is presented in Figure 4.2.

In our event-driven simulator, each event is processed by the event handler and could trigger another event of the same or different type. For example, a traffic arrival event triggers the Msg 1 transmission mechanism at the appropriate UE, which in turn schedules Msg 2 transmission at the eNodeB if Msg 1 has been successful. At the same time, a traffic arrival event causes the formation of another traffic arrival event at the same device based on the traffic arrival patterns discussed above. After Msg 2 reception, Msg 3 transmission is scheduled. This process is repeated until the successful reception of Msg 4, which is enabling the statistics collector. Finally, sorted results are saved into a file that is delivered to a Matlab parser for the purposes of visualization.

4.2.2 Simulation validation

In order to validate our simulation tool against the trustworthy and reliable 3GPP test cases, we have conducted in-depth calibration. In particular, we used the recent reference data approved by 3GPP in the technical report TR 37.868 [23]. In Table 4.2, a comparison between the results from [23] (see e.g. Table 6.2.2.1.1) and our simulation/analysis results are shown for traffic type 1 (uniform activation pattern). The details of our analytical approach will be given in the following section and we include them here only for consistency.

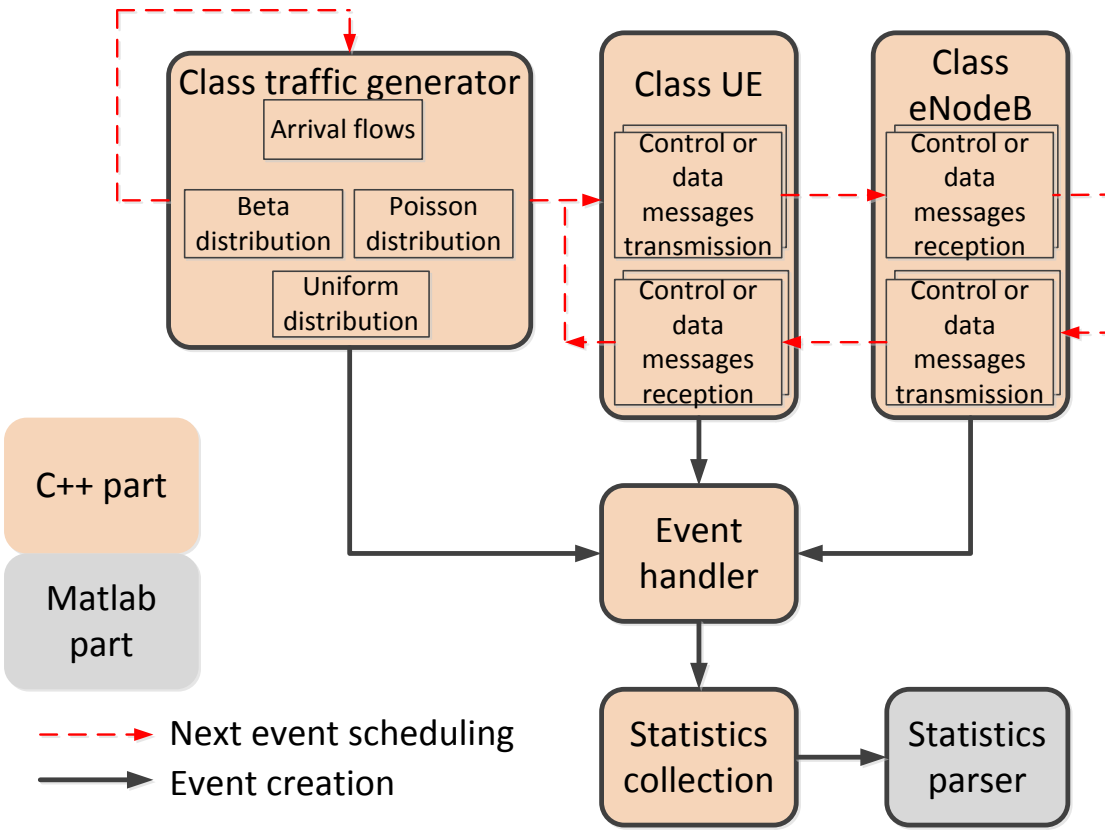

Figure 4.1: Simplified simulator structure.

Table 4.2: Methodology calibration

Number of devices	**5000**	**10000**	**30000**	**Results origin**
Collision Probability (%)	0.01	0.03	0.22	Methodology
	0.01	0.03	0.23	Simulation
Number of preamble	1.43	1.45	1.50	Methodology
	1.43	1.44	1.50	Simulation
Tx attempts	1.44	1.47	1.57	Analysis
Access delay	25.60	26.05	27.35	Methodology
	25.70	26.00	27.10	Simulation
(ms)	25.90	26.40	28.45	Analysis

The Cumulative Distribution Functions (CDFs) of initial network entry delays for 30K MTC devices (both uniform and beta traffic patterns) are presented in Figure 4.3. Importantly, 90% and 10% quantiles agree with the reference values from [23] with less than 15% of difference.

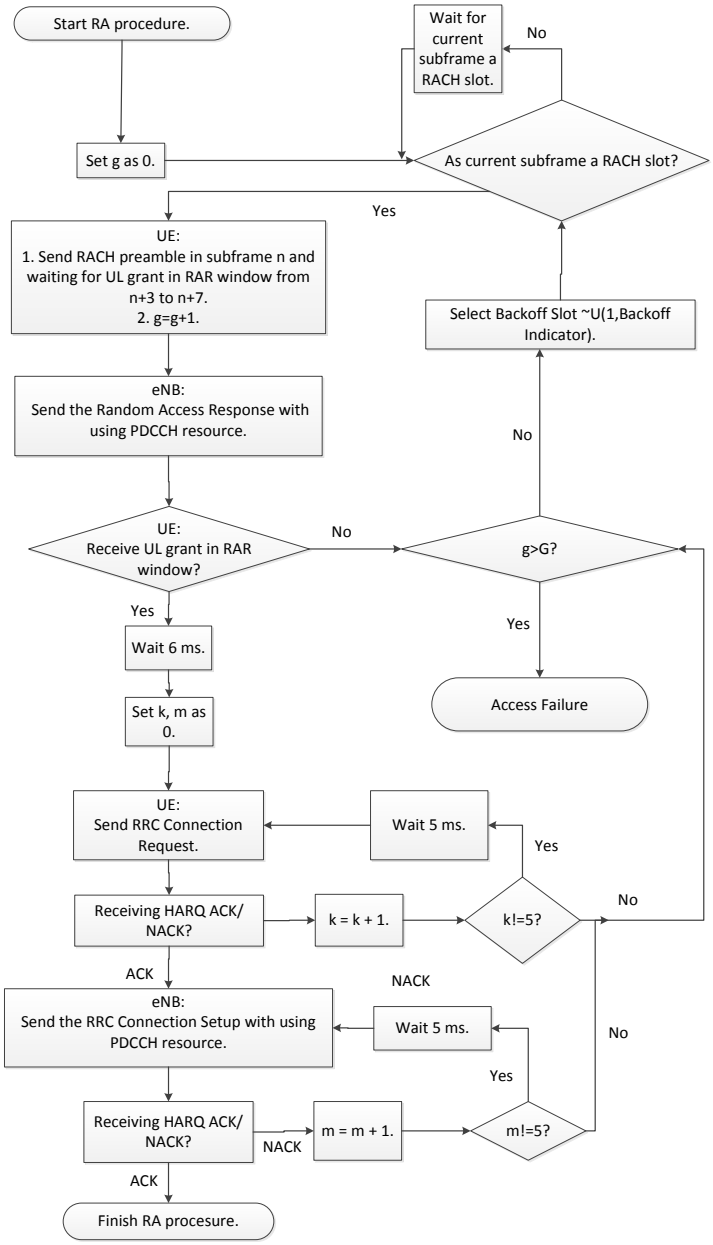

Figure 4.2: Algorithm of system behavior.

4.3 Analytical approach

4.3.1 Delay analysis

In this subsection, we detail our approach to the analytical evaluation of the RACH performance in terms of, primarily, average network access delay. We split the overall delay into two components, corresponding to the Msg 1-2 and Msg 3-4 processing:

$$E[\tau] = E[\tau^{(1)}] + E[\tau^{(2)}], \tag{4.1}$$

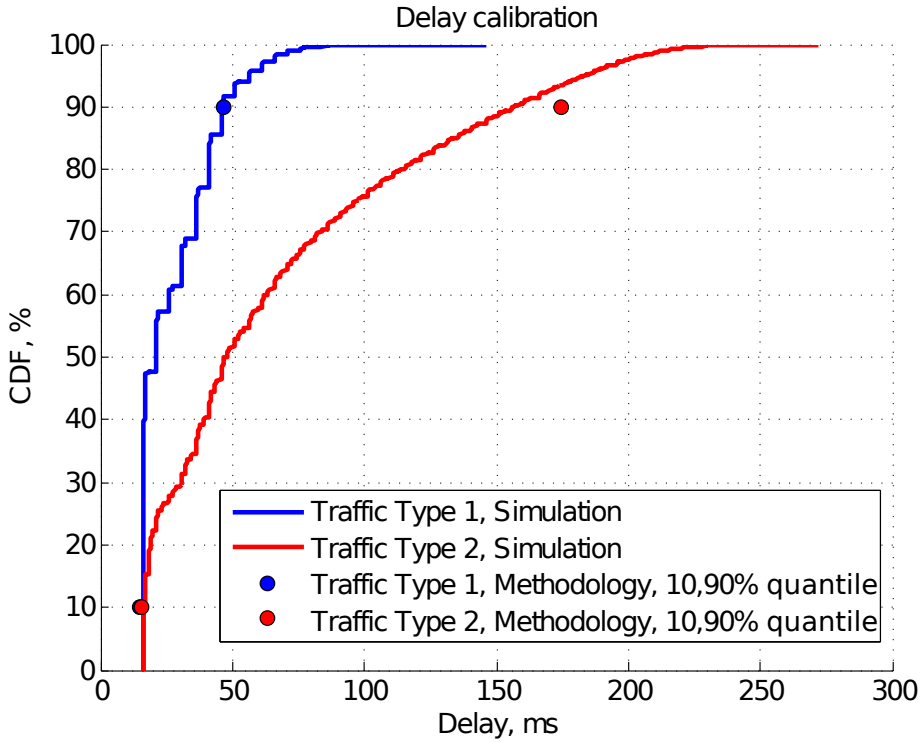

Figure 4.3: Access delay CDF for 30K MTC devices.

where $E[\tau^{(1)}]$ is the time interval between the device activation and the RAR response reception and $E[\tau^{(2)}]$ is the time interval between the end of the subframe when RAR was received and the end of the Msg 4 processing.

The calculation of the distribution and the mean value of the random variable $\tau^{(2)}$ is nearly trivial and the final expression is given as follows:

$$E[\tau^{(2)}] = t_{pr} + \frac{t_{tx}}{\pi_{tx}}\left[1-(1-\pi_{tx})^{L_3}(1+L_3\pi_{tx})\right], \tag{4.2}$$

where parameters t_{pr}, t_{tx} are the processing and Tx timings, $\pi_{tx} = \pi_3\pi_4$ is the probability of successful Msg 3 and Msg 4 transmission, and L_3 is the maximum number of Msg 3 transmission attempts. The following part of our analysis concentrates on the first component of the expression (4.1).

4.3.2 System without collisions

Firstly, we consider the original random-access system without any collisions. Hence, retransmissions occur solely due to the power ramping. In case of successful preamble transmission at the first attempt, the service time consists of preamble transmission time, preamble processing, and the RAR response time. Also we take into account the averaged time between the device activation and the first preamble transmission attempt $b/2$, i.e., $\tau^{(1)} = b/2 + K_1 + K_0 + (K+1)/2$. Here, $(K+1)/2$ stands for the average RAR response time since we assume that the processing starts immediately after receiving the RAR

response.

As mentioned above, the probability of successful preamble transmission at the attempt i is $(1-e^{-i})$ and the complementary probability of the failed transmission is e^{-i}, correspondingly. Further, we average the sum of the backoff time and additional waiting time until the next b-th slot denoting the aggregate value as $\bar{w}$. The distribution of the service time for Msg 1-2 can be given as:

$$Pr\{\tau^{(1)}=\frac{b}{2}+K_1+K_0+(K+1)/2=(1-\frac{1}{e^1}),$$

$$Pr\{\tau^{(1)}=\frac{b}{2}+(K_1+K_0+K+\bar{w})+K_1+K_0+\frac{K+1}{2}\}=\frac{1}{e^1}(1-\frac{1}{e^2})$$

...

$$Pr\{\tau^{(1)}=\frac{b}{2}+(n-1)(K_1+K_0+K+\bar{w})+K_1+K_0+\frac{K+1}{2}\}=\left(1-\frac{1}{e^n}\right)\prod_{i=1}^{n-1}\frac{1}{e^i}$$

...

where $b/2$ stands for the time between the arrival and the beginning of the first preamble transmission attempt, $(K_1+K_0+K+\bar{w})$ is the component, which is added every time when transmission fails. As such, the mean service time before the beginning of Msg 3 Tx is:

$$E[\tau^{(1)}]=(K_1+K_0+K+\bar{w})\sum_{n=1}^{L_3}n\left(1-\frac{1}{e^n}\right)\prod_{i=1}^{n-1}\frac{1}{e^i}+$$

$$+\frac{b-K+1}{2}-\bar{w}=c_1(K_1+K_0+K+\bar{w})+\frac{b-K+1}{2}-\bar{w}, \tag{4.3}$$

where $\bar{w}=c_2(c_2+1)+(c_2+b+bc_3)(W-bc_3-c_2)+bc_3c_2$, $c_1\cong 1.42$, $c_2=b\lceil K/b\rceil-K$, and $c_3=\lfloor(W-c_2)/b\rfloor$. This expression presents a lower bound of $E[\tau^{(1)}]$ for the studied system.

4.3.3 System with collisions

Analysis of the system with collisions constitutes a more challenging task, and an accurate solution is difficult to obtain due to the property of memory as long as the system features random backoff time, constant timings and, especially, large number of preambles. For example, in the classical multi-user system with one preamble, the approximate delay values can easily be obtained as has been done for ALOHA in [43]. For our system, however, the use of that popular technique does not give a good approximation and we thus extend the approach from [44]. In order to abstract away the memory property and establish an estimate for $E[\tau^{(1)}]$ for the system with collisions, we adopt the following equivalent model.

- We assume Bernoulli activation flow with the rate of π, when a device generates a new connection request per subframe with the equivalent probability $\pi = 1/N$, where N is the number of subframes in the original system.

- We omit explicit consideration of the waiting interval and the backoff window replacing them by an assumption that at every subframe a backlogged device activates with a certain probability $\pi_0 = 1/(K_0 + K_1 + K + \bar{w})$. Basically, this means that the device activates once over the period $(K_1 + K_0 + K + \bar{w})$ if the first transmission fails due to a collision or insufficient power.

- The probability of successful departure is μ, i.e. the request is served with a certain probability μ in the current subframe, otherwise the device attempts to access the channel in the next available subframe.

- Finally, we abstract away the maximum number of preamble transmission attempts.

Within the simplified equivalent system model, an approximation of the mean network entry delay may be obtained as follows. For the system without collisions, the probability of being served ($\tilde{\mu}$) can be calculated from the equation $E[\tilde{\tau}^{(1)}] = E[\tau^{(1)}]$ as:

$$\tilde{\mu} = \frac{1}{E[\tau^{(1)}]} = \frac{1}{c_1(K_1+K_0+K+\bar{w}) + \frac{b-K+1}{2} - \bar{w}}, \tag{4.4}$$

where $E[\tau^{(1)}]$ is the mean time interval between the device activation and the RAR reception, whereas $E[\tilde{\tau}^{(1)}]$ is the respective interval in the equivalent model. We will refer to the expression (4.4) in what follows, when calculating the system load for the devices that avoid collisions.

We continue by actually accounting for collisions. Let us consider one subframe and assume that a particular device i has generated a request and also selected a preamble. Let the system be in the state j, where j is the number of backlogged devices including the device i. In the state j, the behavior of the device i can be described by a simple two-state Markov chain, where a state represents the number of pending requests Q_i at the device, which can be equal to either 0 or 1. The transition matrix for the considered chain is given as:

$$\Pi = \begin{pmatrix} 1-\pi & \pi \\ \mu_j & 1-\mu_j \end{pmatrix}. \tag{4.5}$$

As such, the steady-state distribution $\omega = \{\omega_0, \omega_1\}$ can be obtained from the matrix equation $\Pi^T \omega = \omega$, when $\omega_0 + \omega_1 = 1$. Hence, the average number of requests Q_i is expressed as:

$$E[Q_i] = 1 \cdot \omega_1 = \frac{\pi}{\pi + \mu_j}, \tag{4.6}$$

where Q_i is the number of requests at the considered device i and μ_j is the probability of successful preamble transmission.

By the Little's law, we obtain the average time spent by the system in the state j as:

$$E[\tau_j^{(1)}] = \frac{E[Q_i]}{\pi} = \frac{1}{\pi + \mu_j}. \tag{4.7}$$

In the state j, for $j-1$ backlogged devices, the probability of accessing the channel and selecting the same preamble as the device i had is $\pi_0 \cdot 1/s$ (the probability to activate times the probability to select the same preamble). For the inactive $M-j$ devices, the corresponding probability is $\pi \cdot 1/s$ (the probability of arrival in a subframe times the probability to select the same preamble).

Thus, the probability π_j^* to avoid collision for the device i in the state j can be calculated as follows:

$$\pi_j^* = \left(1 - \pi_0 s^{-1}\right)^{j-1} \left(1 - \pi s^{-1}\right)^{M-j}. \tag{4.8}$$

Further, we account for the power ramping effect. The probability to avoid collision at the attempt n is given as follows:

$$Pr\{\text{1st successful}\} = \left(1 - \frac{1}{e}\right)\pi_j^*,$$

$$Pr\{\text{2nd successful}\} = \left(1 - \left(1 - \frac{1}{e}\right)\pi_j^*\right)\left(1 - \frac{1}{e^2}\right)\pi_j^*,$$

$$\ldots$$

$$Pr\{n\text{th successful}\} = \left(1 - \frac{1}{e^n}\right)\pi_j^* \prod_{i=1}^{n-1}\left(1 - \pi_j^*\left(1 - \frac{1}{e^i}\right)\right),$$

$$\ldots.$$

Here, we also neglect all the lost preambles as we did before, averaging by successful transmissions and replacing the sought expectation with the conditional one. The average number of attempts can be obtained as:

$$\bar{n}_j = \pi_j^* \sum_{n=1}^{L_1} n \left(1 - \frac{1}{e^n}\right) \prod_{i=1}^{n-1}\left(1 - \pi_j^*\left(1 - \frac{1}{e^i}\right)\right). \tag{4.9}$$

Taking into account the effect of power ramping, we establish the probability μ_j of successful request i transmission:

$$\mu_j = \left(\bar{n}_j \cdot (K_1 + K_0 + K + \bar{w}) + \frac{b - K + 1}{2} - \bar{w}\right)^{-1}, \tag{4.10}$$

where $\bar{n}_j$ is given by (4.9).

The average service time can then be calculated as:

$$E[\tau^{(1)}] = \sum_{j=1}^{M} \theta_j E[\tau_j^{(1)}] = \sum_{j=1}^{M} \theta_j \frac{1}{\pi + \mu_j}, \tag{4.11}$$

where $\{\theta_j\}_{j=1}^{M}$ is the steady-state distribution, θ_j is the steady-state probability of being in the state j.

In order to obtain the stationary distribution defined above, we need to consider all the state transitions and solve the corresponding matrix equation of dimension M. To reduce the complexity of such calculations, we omit more complicated transitions between the states and average θ_j, using binomial distribution, by:

$$\theta_j = \binom{M-1}{j-1} \rho^{j-1} (1-\rho)^{M-j}, \tag{4.12}$$

where ρ is the device load, and $\binom{M-1}{j-1} = \frac{(M-1)!}{(j-1)!(M-j)!}$.

Here, we disregard all the collisions between other devices by assuming that only the considered device i falls into a collision. Thus, we can calculate the system load $\rho = \pi/\tilde{\mu}$ using the expression (4.4) for the probability of being served μ, derived for the system without collisions.

The resulting expression for the approximate mean service time is:

$$E[\tau^{(1)}] = \sum_{j=1}^{M} \frac{\binom{M-1}{j-1} \rho^{j-1} (1-\rho)^{M-j}}{\frac{1}{N} + \left(a_j(K_1+K_0+K+\vec{w}) + \frac{b-K+1}{2} - \vec{w}\right)^{-1}}, \tag{4.13}$$

where a_j is given above.

4.3.4 Applicability discussion

In this subsection, we emphasize that the proposed analytical approach is applicable only for the practical systems, which can be reduced to a stationary system. This, obviously, can be done when considering the uniform distribution of the device activation time (traffic inter-arrival time) over a fixed time interval.

Otherwise, for instance, in case of beta distribution, one should take into account dynamic changes of the parameters, which is rather tedious and is thus left out of scope of this Thesis.

However, our approach allows for a broad range of important practical extensions. In particular, we can easily analyze a regular MTC operation scenario described further on in Section 5.2, where inter-arrival time follows exponential distribution with a certain parameter $1/\lambda$.

Due to the stationarity of this process, we exploit the same approach and, literally, the

same formulas, while only replacing the probability π with the probability that at least one packet arrives in a particular subframe:

$$\pi = 1 - \Pr\{X(t, t+t_0) = 0\}, \tag{4.14}$$

where t_0 is the size of the subframe, $t_0 = 1$ ms.

In more detail, the data arrival flow constitutes a stationary, ordinary, and memoryless process $\{X(0,t), t \geq 0\} = \{X(t), t \geq 0\}$ representing the number of data arrivals occurred until the moment t:

$$\Pr\{X(t) = k\} = \frac{\lambda^k t^k}{k!} e^{-\lambda t}, k = 0, 1, 2, ..., \tag{4.15}$$

where λ is the arrival flow rate.

Hence, due to the property of stationarity, the probability p_0 that the number of arrivals within a slot of length t_0 equals 0, is given by:

$$\pi = 1 - \Pr\{X(t, t+t_0) = 0\} = 1 - e^{-\lambda t_0}, \tag{4.16}$$

where $X(t, t+t_0)$ is the number of arrivals over the time interval $[t, t+t_0)$, t is an arbitrary time moment, and t_0 is the subframe length.

We finally note that the proposed analytical framework can also incorporate some overload control mechanisms, such as e.g. initial backoff (see Section 5.1 for details). It will produce changes to the equation (4.8) and derivations above concerning the probability to avoid collisions, i.e. the probability to collide should be set to $\pi \cdot \pi_0 \cdot 1/s$ for all $(M - j)$ inactive devices due to the device activation before its first transmission attempt.

4.3.5 Energy consumption analysis

As mentioned previously, our methodology is powerful enough to be extended for the energy-related analysis of the MTC device behavior.

Therefore, we introduce new important parameters (out of scope of [23]), which represent power consumption levels of a typical MTC device. In particular, we consider the maximum of four different device power states (see Figure 2.6):

- P_0 – Inactive State. In this state, the device consumes minimum power. The buffer is empty, no data to transmit.
- P_1 – Idle State. The device is activated, but it does not transmit in the current subframe.
- P_2 – Rx state. The device is expecting Msg 2/Msg 4 or is processing the related responses.

- P_3 – Tx State. The device is transmitting Msg 1/Msg 3. The maximum power is consumed.

We estimate the total energy consumption of a device per subframe as a sum of fractions of time spent in every power state multiplied by the power consumption in the corresponding state. Therefore, we analytically establish the time spent by the device in every of four possible power states by calculating the corresponding time proportions as follows.

Tx state time is given by:

$$q_3 = K_1\bar{n} + \frac{1}{\pi_{tx}}\left[1-(1-\pi_{tx})^{L_3}(1+L_3\pi_{tx})\right], \tag{4.17}$$

where $\bar{n}$ is the estimation for the mean number of preamble transmission attempts and $K_1\bar{n}$ corresponds to the time of preamble transmission, while the second part accounts for the average number of Msg 3 transmissions.

Rx state time is given as:

$$q_2 = K(\bar{n}-1) + \frac{K+1}{2} + t_{pr} + \frac{t_{tx}-1}{\pi_{tx}}\left[1-(1-\pi_{tx})^{L_3}(1+L_3\pi_{tx})\right], \tag{4.18}$$

where $K(\bar{n}-1)$ is the time spent expecting the RAR response, $(K+1)/2$ is the mean index of the response from eNodeB at the successful attempt, and the remainder corresponds to the processing and receiving of Msg 3 and Msg 4.

Idle state time can be calculated as:

$$q_1 = \frac{b}{2} + K_0\bar{n} + (\bar{n}-1)\bar{w}, \tag{4.19}$$

where $K_0\bar{n}$ is the time for the eNodeB to process the preamble after its reception and $\frac{b}{2}$ is the idle time between the activation and the beginning of the preamble transmission.

The approximate average number of transmissions for the mean number of preamble transmission attempts is given by the formula:

$$\bar{n} = \sum_{j=1}^{M}\binom{M-1}{j-1}\rho^{j-1}(1-\rho)^{M-j}\pi_j^* \cdot a_j. \tag{4.20}$$

Finally, the estimated total energy expenditure of an MTC device can be calculated as:

$$\varepsilon = P_0(N-q_3-q_2-q_1)+P_1q_1+P_2q_2+P_3q_3. \tag{4.21}$$

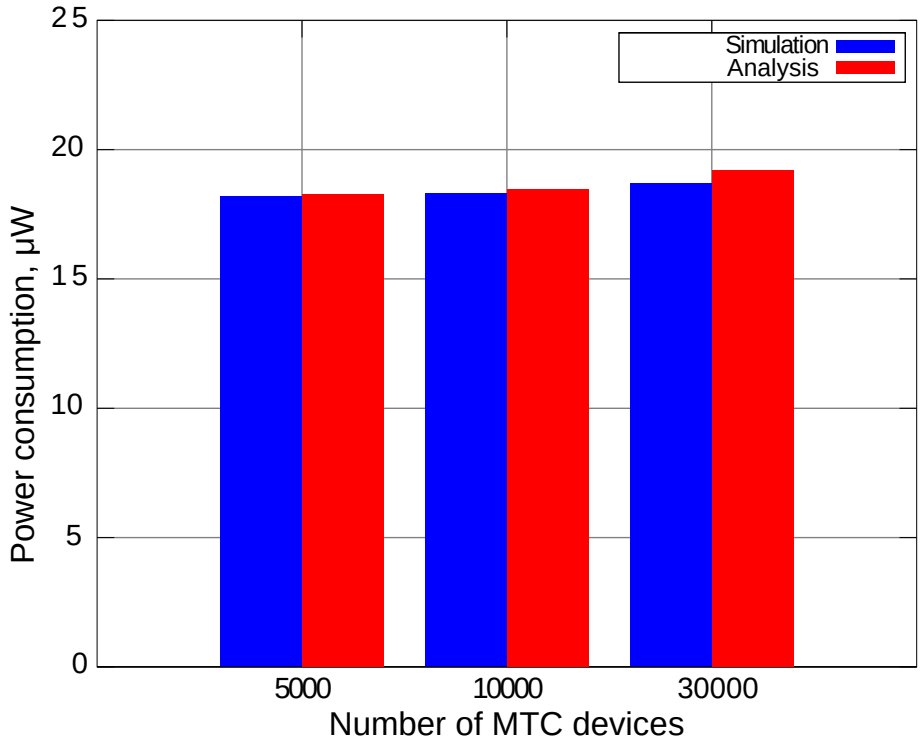

Figure 4.4: RA power consumption.

The analytical and simulation results for the MTC device power consumption (traffic type 1, uniform) are summarized in Figure 4.4. We notice that the provided analytical approximation is extremely accurate even when the population of MTC devices is high.

5. NUMERICAL RESULTS & CONCLUSIONS

Possible solutions and their analysis for the considered problems are described in this Chapter. Here, the emphasis is made on the energy efficiency and power consumption results. However, the conventions metrics, calibrated in the previous Chapter are also targeted. In the end of the Chapter, we are also discussing the results and showing possible future directions of the research.

5.1 MTC Overload conditions

Our evaluation framework detailed above may be used to conclude on the feasibility of the candidate RAN overload control solutions (see e.g., [22]). In particular, we consider a combination of initial back-off (pre-backoff) proposed by [45] and MTC-specific back-off described in [46]. The main idea is that the backoff time is invoked not only after any unsuccessful preamble transmission attempt, but also at the very beginning of every RA procedure to de-correlate the surge in channel access attempts from many MTC devices. As a result, with a large enough BI value chosen, the network entry peaks can be smoothened and the collision probability may be decreased. Given that many MTC applications are delay-tolerant, some increase in the mean access delay is often acceptable.

To conclude on this study item, we have performed simulations based on traffic type 2 (beta distribution, more correlated entry attempts). In Figures 5.1, 5.2 , collision probability, and access success probability for different BI values (which may also be larger than those currently defined by the LTE-A specification) were evaluated.

In this figure, the BI starts from 20 ms and is increased up to its maximum standardized value of 960 ms [30]. As can be seen from the plot, access success probability after all the available retries is about 80%, which may not be acceptable for many MTC-aware scenarios. Therefore, we consider the use of the three reserved options for the BI in [30] with larger values: 1920, 3840, and 7680 ms. As a result, additional delay is compensated by a considerably higher (up to 100%) reliability level of the network access.

5.2 Regular operation conditions

By contrast to the previous (sub)sections focusing on the case of MTC overload, this subsection concentrates on regular MTC operation when all the devices have already performed their initial network entry. The LTE-A specification allows the use of PRACH for scheduling request transmission, whenever the device does not have the resources

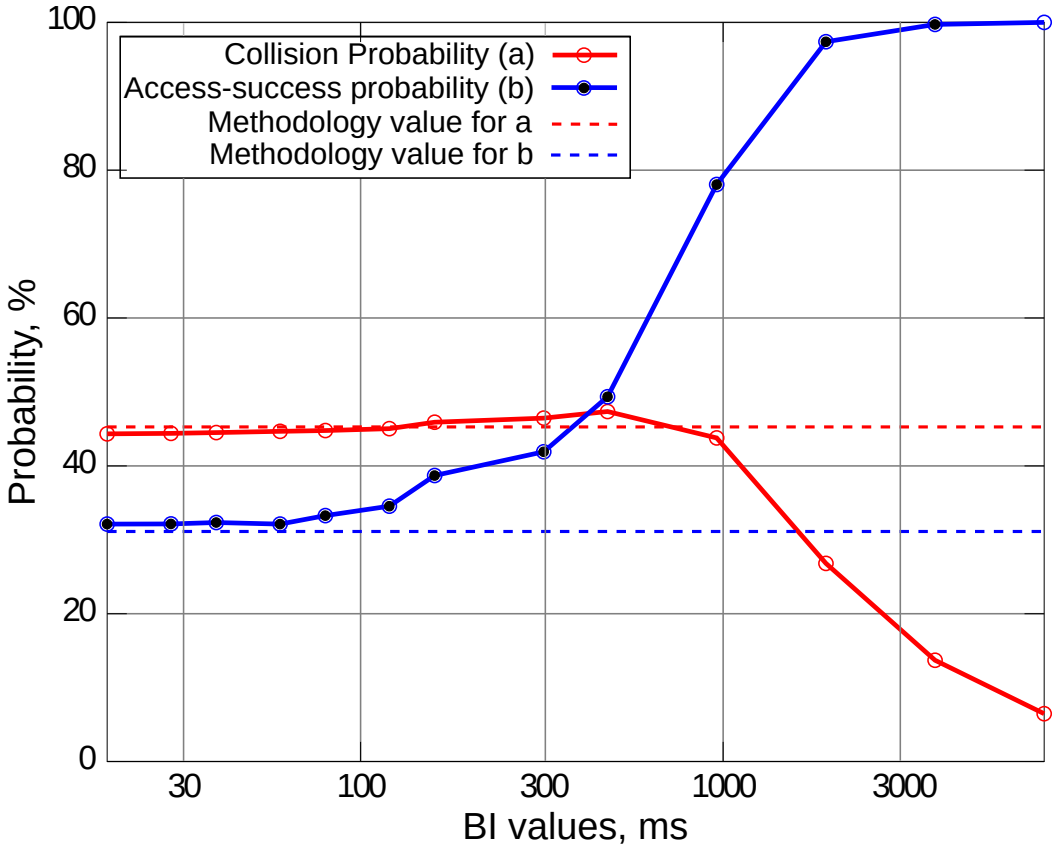

Figure 5.1: Overload control performance: collision probability, and access success probability

allocated over the default control channel [30]. However, the methodology in [23] defines only overloaded network entry patterns leaving open the actual device traffic model. Therefore, below we consider the reference MTC UL traffic model in accordance with the recent 3GPP technical report [47].

The document [47] suggests that the packet inter-arrival time distribution is exponential with the constant mean value of 30 seconds and alternative packet sizes of 256 and 1024 bits. Conventional metrics are not so interesting in this case, because they will be close to normal values. However, since in the considered scenario the MTC devices send actual data, we may explicitly account for their energy efficiency. Energy efficiency may be calculated as the number of data packets that were transmitted successfully by a device, weighted with the packet size, and related to the total energy (in Joules) spent by this device. Consequently, the dimension of this important metric is bits per Joule (bpJ).

Both simulation results and our analysis (obtained by extending the proposed approach from the previous section) are shown in Figure 5.3. Noteworthy, the device energy efficiency is changing insignificantly with the overall population of the MTC devices. This is due to the fact that the actual MTC device energy efficiency is quite low when compared to e.g., a typical mobile device [48] and has significant potential for further improvement. Finally, we conclude that the analytical results are very close to the simulated values. The

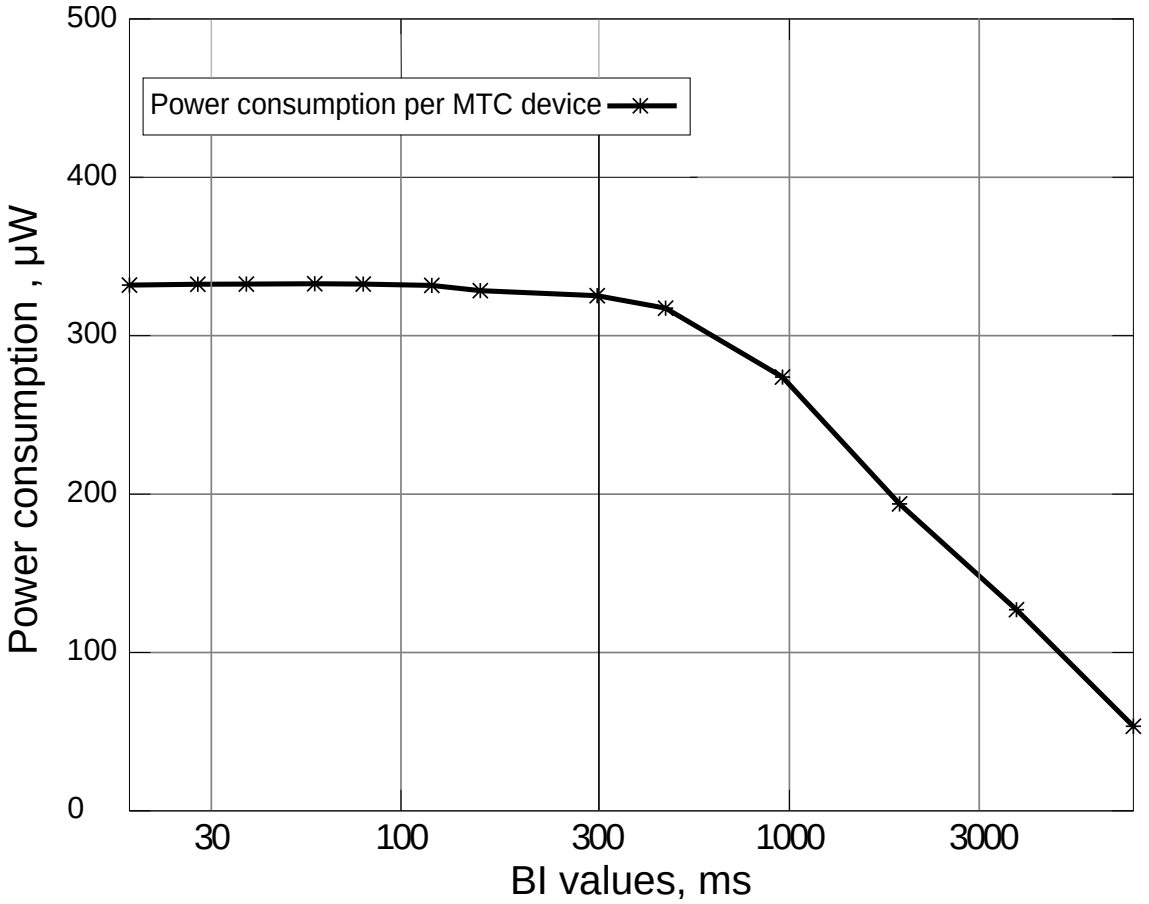

Figure 5.2: Overload control performance: power consumption

only notable difference could be seen for 30K devices due to a slightly decreased accuracy of our analytical approach for higher traffic arrival rates.

5.3 Conclusions and possible extensions

In this Thesis we emphasized the lack of comprehensive evaluation frameworks for the performance assessment of the PRACH mechanism within the 3GPP LTE-A technology that would rely on both simulation and analysis components. Moreover, previous evaluation results are often disjoint and contradictory due to the fact that the unified 3GPP calibration methodology has only been finalized very recently. As such, we have accounted for the latest reference data approved by 3GPP while validating our own advanced protocol-level RACH simulator.

In Chapter 3 we have also made a complete analysis of currently existing simulation tools, which are frequently used in practice as core instrument to predict the future network behavior. In general, this overview was very useful in the process of creation of our own simulation tool. However, the modern wireless communication oriented research could not always relies only on the simulations, therefore powerful and flexible analytical instrument was applied and calibrated.

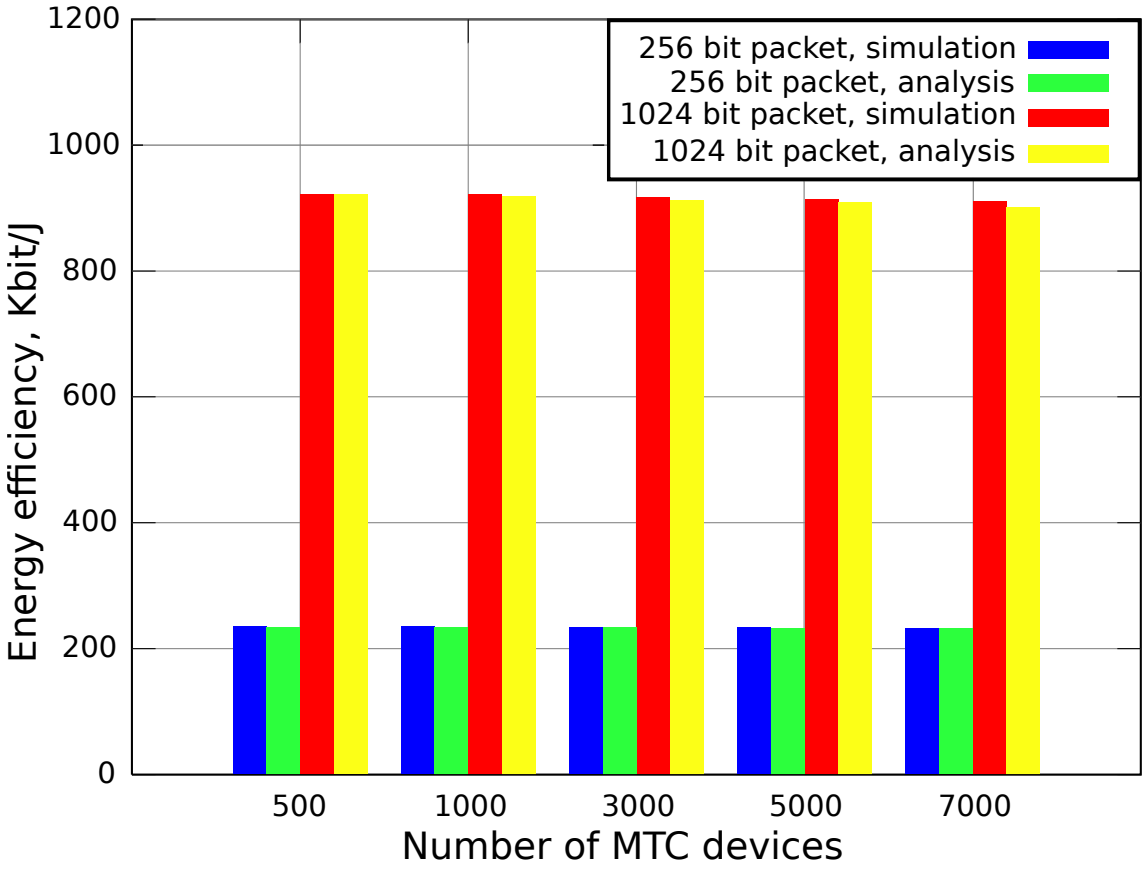

Figure 5.3: Regular MTC operation performance.

Further, we conducted an in-depth analysis of the case when the RAN is facing a surge in near-simultaneous network entry attempts from an excessive number of MTC devices. To add even more insight to the MTC device behavior, we also considered the regular device operation, when initial network entry has already been performed and the device is sending its actual UL data. Our approach allows to investigate the performance of MTC devices, the impact of PRACH settings, and the overload control mechanisms in terms of conventional metrics, such as access success probability and medium access delay. In particular, the limitation of existing access protocol in case of correlated network entry attempts has been indicated and the benefits of several potential enhancements were highlighted. These modifications do not require major protocol change and feature the pre-backoff technique complemented by the usage of larger MTC-specific BI values. Moreover, the analytical technique presented in this Thesis is a powerful tool that can be used to extend the 3GPP RACH calibration methodology [23]. One such improvement accounts for the power-related metrics of an MTC device to conclude on all the aspects of the random access procedure, including its energy efficiency. Furthermore, based on the research made in this Thesis, a new energy and resource efficient contention-based mechanism was considered and analyzed in [3].

Our estimation of delay and power consumption has been found to be very accurate

and we plan to work on it further considering additional realistic features of RACH performance. Our analytical approach is also applicable for studying other MTC-related enhancements within LTE-A, such as sending scheduling requests via PUCCH, Extended Access Barring (EAB, [49]) scheme, and Extended Wait Timer (eWaitTimer, [50]) mechanism.

REFERENCES

[1] Mikhail Gerasimenko, Sergey Andreev, Yevgeni Koucheryavy, Alexey Trushanin, Vyacheslav Shumilov, Michael Shashanov, and Sergey Sosnin. Performance Comparison of System Level Simulators for 3GPP LTE Uplink. In *12th International Conference, NEW2AN 2012*, pages 186–197, St. Petersburg, Russia, 2012.

[2] Mikhail Gerasimenko, Vitaly Petrov, Olga Galinina, Sergey Andreev, and Yevgeni Koucheryavy. Energy and Delay Analysis of LTE-Advanced RACH Performance under MTC Overload. In *IEEE Globecom 2012 Workshops (GC Wkshps)*, pages 1632 – 1637, Anaheim, USA, 2012.

[3] Sergey Andreev, Anna Larmo, Mikhail Gerasimenko, Vitaly Petrov, Olga Galinina, Tuomas Tirronen, Johan Torsner, and Yevgeni Koucheryavy. Efficient Small Data Access for Machine-Type Communications in LTE. In *IEEE ICC 2013 Next-Generation Networking Symposium*, pages 3544–3549, Budapest, Hungary, 2013.

[4] Mikhail Gerasimenko, Vitaly Petrov, Olga Galinina, Sergey Andreev, and Yevgeni Koucheryavy. Impact of MTC on Energy and Delay Performance of Random-Access Channel in LTE-Advanced. *Transactions on Emerging Telecommunications Technologies*, 24(4):366–377, June 2013.

[5] Harbor Research Report. *Machine-To-Machine (M2M) & Smart Systems Forecast 2010-2014*, 2009.

[6] Bob Emmerson. *M2M: the Internet of 50 billion devices*, January 2010.

[7] Geng Wu, Shilpa Talwar, Kerstin Johnsson, Nageen Himayat, and Kevin D. Johnson. M2M: from Mobile to Embedded Internet. *IEEE Commun. Mag.*, 49(4):36–43, April 2011.

[8] ETSI Technical Specification (TS) 102 689 v 1.1.1. Machine-to-Machine communications (M2M); M2M service requirements, 2010.

[9] HanGyu Cho and Jose Puthenkulam. IEEE 802.16ppc-10/0002r6. Machine to Machine (M2M) Communication Study Report. Technical report, 2010.

[10] Nageen Himayat, Shilpa Talwar, Kerstin Johnsson, Shantidev Mohanty, Xinrong Wang, Grace Wei, Eve Schooler, George Goodman, Sergey Andreev, Olga Galinina, and Turlikov Andrey. IEEE C802.16p-10/0007r1. Informative text on Smart Grid applications for inclusion in IEEE 802.16p Systems Requirements Document (SRD). 2010.

[11] Sergey Andreev, Olga Galinina, and Yevgeni Koucheryavy. Energy-Efficient Client Relay Scheme for Machine-to-Machine Communication. In *Proc. of the 54th Global Communications Conference (GLOBECOM)*, pages 1–5, Houston, TX, USA, 2011.

[12] 3GPP Technical Report (TR) 23.888 v1.6.0. System Improvements for Machine-Type Communications, 2011.

[13] 3GPP Technical Report (TR) 22.888 v0.7.0. Study on enhancements for MTC, 2012.

[14] 3GPP Technical Report (TR) 23.887. Machine-Type and other Mobile Data Applications Communications Enhancements, 2012.

[15] Ivan N. Vukovic. Throughput Comparison of Random Access Schemes in 3GPP. In *Vehicular Technology conference (VTC 2003)*, volume 1, pages 616–620, Orlando, Florida, USA, 2003.

[16] Yang Yangn and Tak-Shing Peter Yum. Analysis of random access channel in UTRA-TDD on AWGN channel. *Internetional journal of communication systems*, 17(3):180–192, April 2004.

[17] Yang Yang and Tak-Shing Peter Yum. Analysis of Power Ramping Schemes for UTRA-FDD Random Access Channel. *IEEE transactions on wireless communications*, 4(6):2688–2693, November 2005.

[18] Insoo Koo, Seokjoo Shin, and Kiseon Kim. Performance Analysis of Random Access Channel in OFDMA Systems. *Proceedings of the 2005 Systems Communications*, pages 128 – 133, 2005.

[19] Ping Zhou, Honglin Hu, Haifeng Wang, and Hsiao-Hwa Chen. An Efficient Random Access Scheme for OFDMA Systems with Implicit Message Transmission. *IEEE transactions on wireless communications*, 7(7):2790–2797, 2008.

[20] Shao-Yu Lien, Kwang-Cheng Chen, and Yonghua Lin. Toward Ubiquitous Massive Accesses in 3GPP Machine-to-Machine Communications. *IEEE Communications Magazine*, 49(4):66–74, 2011.

[21] Ki-Dong Lee, Sang Kim, and Yi Byung. Throughput Comparison of Random Access Methods for M2M Service over LTE Networks. In *GLOBECOM International Workshop on Machine-to-Machine Communications*, pages 373 – 377, Houston, TX, USA, 2011.

[22] Ming-Yuan Cheng, Guan-Yu Lin, Hung-Yu Wei, and Hsu A.C.-C. Overload Control for Machine-Type-Communications in LTE-Advanced System. *IEEE Communications Magazine Mag.*, 50(6):38–45, June 2012.

[23] 3GPP Technical Report (TR) 37.868. Study on RAN Improvements for Machine-Type Communications, 2011.

[24] Kan Zheng, Fanglong Hu, Wenbo Wang, Wei Xiang, and Mischa Dohler. Radio Resource Allocation in LTE-Advanced Cellular Networks with M2M Communications. *IEEE Communications Magazine*, 50(7):184–192, July 2012.

[25] Dusit Niyato, Lu Xiao, and Ping Wang. Machine-to-Machine Communications for Home Energy Management System in Smart Grid. *IEEE Communications Magazine*, 49(4):53–59, April 2011.

[26] UTRA-UTRAN Long Term Evolution (LTE) and 3GPP System Architecture Evolution (SAE). Technical report, 3GPP.

[27] 3GPP Technical Specification (TS) 36.211. Physical Channels and Modulation, 2012.

[28] 3GPP Technical Specification (TS) 36.213. Physical layer procedures, 2012.

[29] 3GPP Technical Report (TR) 36.822. LTE Radio Access Network (RAN) enhancements for diverse data applications, 2012.

[30] 3GPP Technical Specification (TS) 36.321. Evolved Universal Terrestrial Radio Access (E-UTRA); Medium Access Control (MAC) protocol specification, 2012.

[31] Chris Johnson. *Long Term Evaluation IN BULLETS*. CreateSpace Independent Publishing Platform, 1st edition, 2010.

[32] A. Maeder, P. Rost, and D. Staehle. The Challenge of M2M Communications for the Cellular Radio Access Network. *11th Würzburg Workshop on IP: Joint ITG and Euro-NF Workshop "Visions of Future Generation Networks" (EuroView2011)*, 2011.

[33] Opnet website. Available at: http://www.opnet.com/.

[34] Omnet ++ website. Available at: http://www.omnetpp.org/.

[35] NS2 website. Available at: http://www.isi.edu/nsnam/ns/.

[36] NS3 website. Available at: http://www.nsnam.org/.

[37] GNS website. Available at: http://www.gns3.net/.

[38] Hurricane 2 website: http://www.packetstorm.com/psc/psc.nsf/site/Hurricane-II-software/.

[39] Natalia Vassileva, Yevgeni Koucheryavy, and Francisco Barcelo-Arroyo. Guard Capacity Implementation in Opnet Modeler WiMAX Suite. *Ultra Modern Telecommunications & Workshops, 2009. ICUMT '09. International Conference on*, pages 1–6, 2009.

[40] Alexander Maltsev, Alexey Khoryaev, Roman Maslennikov, Mikhail Shilov, Maxim Bovykin, Gregory Morozov, Andrey Chervyakov, Andrey Pudeyev, Vadim Sergeyev, and Alexey Davydov. Analysis of IEEE 802.16m and 3GPP LTE Release 10 Technologies by Russian Evaluation Group for IMT-Advanced. *International Congress on Ultra Modern Telecommunications and Control Systems and Workshops (ICUMT)*, pages 901–908, 2010.

[41] 3GPP Technical Report (TR) 36.912. Feasibility study for Further Advancements for E-UTRA (LTE-Advanced), 2012.

[42] Mischa Dohler, Thomas Watteyne, and Jesús Alonso-Zárate. *Machine-to-Machine An Emerging Communication Paradigm*, 2010.

[43] Leonard Kleinrock and Simon S. Lam. Packet-Switching in a Multi-Access Broadcast Channel: Performance Evaluation. *IEEE Transactions on Communications*, COM-23(4):410–423, April 1975.

[44] M. Sidi and A. Segall. Two Interfering Queues in Packet-Radio Networks. *IEEE Transactions on Communications*, 31(1):123–129, January 1983.

[45] 3GPP TSG-RAN WG2 Meeting 74. R2-113013. Access barring for delay tolerant access in LTE, 2011.

[46] 3GPP TSG RAN WG2 73bis R2-112863. Backoff enhancements for RAN overload control, 2011.

[47] 3GPP Technical Report (TR) 36.888. Study on provision of low-cost MTC UEs based on LTE, 2012.

[48] Sergey Andreev, Pavel Gonchukov, Nageen Himayat, Yevgeni Koucheryavy, and Andrey Turlikov. Energy efficient communications for future broadband cellular networks. *Computer Communications Journal (COMCOM)*, 35(14):1662–1671, August 2012.

[49] Jen-Po Cheng, Chia-han Lee, and Tzu-Ming Lin. Prioritized Random Access with dynamic access barring for RAN overload in 3GPP LTE-A networks. *GLOBECOM Workshops (GC Wkshps)*, pages 368 – 372, 2011.

[50] 3GPP TSG-RAN WG2 73bis R2-112202. Discussion on the UE behaviour when receiving the eWaitTime in LTE., 2011.